



HAL
open science

Testing the performance of dendroclimatic process-based models at global scale with the PAGES2k tree-ring width database

Jeanne Rezsöhazy, Fabio Gennaretti, Hugues Goosse, Joël Guiot

► To cite this version:

Jeanne Rezsöhazy, Fabio Gennaretti, Hugues Goosse, Joël Guiot. Testing the performance of dendroclimatic process-based models at global scale with the PAGES2k tree-ring width database. *Climate Dynamics*, 2021, 10.1007/s00382-021-05789-7 . hal-03252700

HAL Id: hal-03252700

<https://hal.science/hal-03252700>

Submitted on 8 Jun 2021

HAL is a multi-disciplinary open access archive for the deposit and dissemination of scientific research documents, whether they are published or not. The documents may come from teaching and research institutions in France or abroad, or from public or private research centers.

L'archive ouverte pluridisciplinaire **HAL**, est destinée au dépôt et à la diffusion de documents scientifiques de niveau recherche, publiés ou non, émanant des établissements d'enseignement et de recherche français ou étrangers, des laboratoires publics ou privés.

Testing the performance of dendroclimatic process-based models at global scale with the PAGES2k tree-ring width database

Jeanne Rezsöhazy · Fabio Gennaretti ·
Hugues Goosse · Joël Guiot

Received: date / Accepted: date

1 **Abstract** Tree-rings are one of the most commonly used proxies for recon-
2 structing past climates at annual resolution. The climate information is gen-
3 erally deduced from tree-rings using statistical relationships, but the assumed
4 linearity and stationarity may be inadequate. Process-based models allow for
5 non-stationarity and non-linearity; however, many challenges are associated
6 with their application for global scale reconstructions. In this study, we aim
7 to test the feasibility of using the mechanistic model MAIDEN at the global
8 scale for paleoclimate data assimilation based reconstructions by applying it
9 to the PAGES2k tree-ring width database. We also compare its performance
10 with the simpler model VS-Lite, often used in global applications. Both mod-
11 els are skillful in terms of calibration and verification correlations for a similar
12 number of sites (63 and 64 for VS-Lite and MAIDEN, respectively). VS-Lite
13 tends to perform better for sites where the climate signal in tree-rings is strong
14 and clear. By contrast, MAIDEN's performance is likely mostly limited by the

J. Rezsöhazy

Université catholique de Louvain (UCLouvain), Earth and Life Institute (ELI), Georges
Lemaître Centre for Earth and Climate Research (TECLIM), Place Louis Pasteur, B-1348
Louvain-la-Neuve, Belgium

Aix Marseille University, CNRS, IRD, INRA, Collège de France, CEREGE, Aix-en-Provence,
France

Tel.: +32 10 47 92 58

E-mail: jeanne.rezsohazy@uclouvain.be

F. Gennaretti

Institut de recherche sur les forêts, UQAT, Amos, Québec, J9T 2L8, Canada

H. Goosse

Université catholique de Louvain (UCLouvain), Earth and Life Institute (ELI), Georges
Lemaître Centre for Earth and Climate Research (TECLIM), Place Louis Pasteur, B-1348
Louvain-la-Neuve, Belgium

J. Guiot

Aix Marseille University, CNRS, IRD, INRA, Collège de France, CEREGE, Aix-en-Provence,
France

15 lack of data (for example, daily Gross Primary Production data or pheno-
16 logical timings) needed to accurately calibrate the model. However, when the
17 calibration is robust, both models reproduce well the observed link between
18 climate and tree-growth. In general, VS-Lite tends to overestimate the climate
19 signal in tree-rings compared to MAIDEN, which better reproduces the mag-
20 nitude of the climate signal on average. Our results show that both models
21 are complementary and can be applied at the global scale to reconstruct past
22 climates using an adequate protocol designed to exploit existing tree-ring data.

23 **Keywords** Ecophysiological modelling · Proxy system models · Dendrocli-
24 matology · PAGES2k tree-ring database · Paleoclimate data assimilation
25 based reconstructions

26 1 Introduction

27 Studying past climates prior to the instrumental period requires the use of in-
28 direct records of climate variations from natural archives, commonly referred
29 to as proxies (Jones et al., 2009). Different projects and consortia have emerged
30 in recent years to improve global climate reconstructions using the develop-
31 ment of global multi-proxy databases spanning last millennium (PAGES 2k
32 Consortium, 2013; Wilson et al., 2016; Anchukaitis et al., 2017; PAGES 2k
33 Consortium, 2017; Tardif et al., 2019; Konecky et al., 2020). Among avail-
34 able records, tree-rings are one of the most commonly used proxies for recon-
35 structing past climates at high temporal (annual) resolution, due to their large
36 spatial coverage and availability (Fritts, 1976; Jones et al., 2009; Mann et al.,
37 2009; Wilson et al., 2016; Anchukaitis et al., 2017; Esper et al., 2018; Anderson
38 et al., 2019; St. George and Esper, 2019).

39 To make the link between climate and indirect observations of paleocli-
40 mate variations from proxies, proxy system models (PSMs; i.e. models that
41 simulate the development of measured variables, for example tree-ring width,
42 in response to a climate forcing; Evans et al., 2013; Dee et al., 2016) must be
43 used. Such models can be applied in the forward mode, for example to compare
44 proxy data directly with climate model simulations when these simulations are
45 used as inputs of the PSM. In the inverse mode, PSMs can reconstruct the
46 climate variations that produce the measured variables (Guiot et al., 2000;
47 Evans et al., 2013).

48 In the case of tree-growth proxy data (such as tree-ring width, hereafter
49 TRW, or density), the climate information is generally deduced on the ba-
50 sis of a statistical relationship calibrated over the instrumental period (Fritts,
51 1976; Cook and Kairiukstis, 1990; Fritts, 1991; Jones et al., 1998; Mann et al.,
52 1999, 2008). Therefore, many climate reconstructions of the period covered by
53 dendroclimatic data have been developed with linear regressions between cli-
54 mate variables and proxy records (Fritts, 1991; Jones et al., 1998; Mann et al.,
55 1999, 2008). This raises concern about the assumed linearity and stationarity
56 of the relationship deduced from the calibration (Briffa et al., 1998; Wilson and
57 Elling, 2004; Wilson et al., 2007; D'Arrigo et al., 2008; Guiot et al., 2014). A

58 complementary approach that has been expanded over the past decade is data
59 assimilation, which combines information from the physics of the system in-
60 cluded in climate models and indirect climate observations provided by proxy
61 data, such as TRW (e.g. Goosse et al., 2012; Franke et al., 2017; Steiger et al.,
62 2018; Tardif et al., 2019). So far, the studies using tree-ring proxy data with
63 data assimilation have focused on the use of statistical PSMs (i.e., univariate
64 or multiple linear regressions) to provide a large-scale reconstruction over the
65 past millennia (e.g. Tardif et al., 2019).

66 As a complement to statistical methods, the link between climate and
67 tree-ring proxy data can be established from process-based PSMs. Mechanistic
68 modelling of tree-growth dependency on climate explicitly states the processes
69 that govern the relationship between climate and tree-growth and allows for
70 non-stationarity and non-linearity (Guiot et al., 2014). While in regression-
71 based PSMs, tree-growth is assumed to be only dependent on the chosen cli-
72 mate target variables, mechanistic modelling introduces the influence of other
73 climate variables, for example atmospheric CO₂ concentration. Additionally,
74 tree-ring-based reconstructions are often limited to sites where tree-growth is
75 driven by one limiting climatic factor. Yet, process-based tree-growth models
76 are able to extract a climate signal from tree-rings at sites where tree-growth is
77 driven by multiple climatic factors. Accordingly, they may expand the area of
78 dendroclimatic reconstructions to a wide range of regions away from extreme
79 growth environments (Breitenmoser et al., 2014; Babst et al., 2018). To date,
80 such models have only been used for local reconstructions (e.g. Boucher et al.,
81 2014). While global scale reconstructions are theoretically possible with a data
82 assimilation procedure including a process-based PSM, such models have only
83 been applied in a pseudo-proxy context (Dee et al., 2016; Acevedo et al., 2017;
84 Steiger and Smerdon, 2017). A further step would be to introduce such mech-
85 anistic models in the data assimilation procedure using actual proxy data to
86 possibly improve the quality of the reconstruction.

87 However, many challenges are associated with the use of process-based
88 tree-ring PSMs for global scale reconstructions. In particular, the inclusion of
89 complex biological processes, for example photosynthesis and carbon alloca-
90 tion, usually implies a cautious initialization and calibration of the model at
91 each particular site of interest, depending on the site environment or the tree
92 species. This information is not readily available at global coverage with the
93 necessary detail. Running and calibration time of such models can also be an
94 obstacle to their utilization.

95 Among the many available process-based dendroclimatic models, the Vaganov-
96 Shashkin-Lite model (VS-Lite; Tolwinski-Ward et al., 2011) has been used in
97 several paleoclimate studies (Breitenmoser et al., 2014; Lavergne et al., 2015;
98 Dee et al., 2016; Steiger and Smerdon, 2017; Seftigen et al., 2018; Fang and
99 Li, 2019). The model is not considered as fully mechanistic. Indeed, VS-Lite
100 does not include any explicit representation of tree-growth processes, but re-
101 lies instead on the principle of limiting factors (soil moisture and temperature;
102 Tolwinski-Ward et al., 2011) to mimic the response of tree-ring growth to cli-
103 mate conditions. The model has faced difficulties in simulating tree-growth

104 where the dependence on climate is not dominated by a limiting factor, such
105 as precipitation or temperature (Breitenmoser et al., 2014).

106 Process-based dendroclimatic models that describe more mechanistically
107 the response of proxy data to climate could overcome those limitations. Among
108 the complex mechanistic models (e.g. Misson, 2004; Dufrêne et al., 2005;
109 Vaganov et al., 2006; Drew et al., 2010), we will focus here on the model
110 MAIDEN (Modelling and Analysis In DENdroecology; Misson, 2004) that
111 explicitly includes biological processes and has the potential to be applied
112 at the global scale. Unlike VS-Lite, MAIDEN also takes into account atmo-
113 spheric CO₂ concentration as an input, allowing the user to consider the non-
114 stationary dependency of tree-growth on the recent exponential increase of
115 CO₂ (Myhre et al., 2013; Boucher et al., 2014). Another important difference
116 between MAIDEN and VS-Lite is the theoretical basis of the models. VS-Lite
117 is a "sink" model in the sense that it only considers the climate constraints on
118 tree-rings (the carbon sink tissues at the tree-level; see Körner, 2015; Fatichi
119 et al., 2014, 2019). MAIDEN is a "source-sink" mechanistic model in the sense
120 that it first determines the carbon availability by modelling photosynthesis,
121 and second, it allocates the available carbon to the sink tissues based on allo-
122 cation and climate-dependent rules. Feedbacks between allocation and photo-
123 synthesis are also considered in MAIDEN. So far, MAIDEN has been applied
124 to the European temperate forests (Misson, 2004; Boucher et al., 2014), to
125 the Mediterranean forests (Gea-Izquierdo et al., 2015, 2017), to the eastern
126 Canadian taiga (Gennaretti et al., 2017) and to Argentine forests (Lavergne
127 et al., 2017). However, unlike VS-Lite, MAIDEN has not been applied at the
128 global scale yet, due to its level of complexity. In particular, the need for daily
129 climate data at high spatial resolution and for measurements of ecophysiological
130 variables to calibrate the model parameters represents the main limitation
131 for its systematic application in different regions. In Rezsöhazy et al. (2020), a
132 protocol has been developed to calibrate and apply MAIDEN automatically at
133 any site globally that contains TRW observations in the extratropical regions.

134 To date, the new protocol applying MAIDEN globally has not been demon-
135 strated. To this end, this study highlights the advantages and potential limita-
136 tions of using a process-based model like MAIDEN at the global scale. In the
137 future, such mechanistic PSM could be utilized for paleoclimate data assimi-
138 lation based reconstructions. Specifically, we perform a comparative analysis
139 of the performance of the simpler VS-Lite and the more complex MAIDEN
140 process-based models. Both models have been applied over the last century to
141 the global TRW data network of PAGES2k (PAGES 2k Consortium, 2017),
142 including 354 TRW records. Studies such as this which lend insight into the
143 mechanisms controlling tree-ring width and tree-growth elevate our ability to
144 extract meaningful climate information from tree-ring networks. This informa-
145 tion is required to improve our understanding of natural and forced decadal
146 climate variability, and to potentially improve reconstructions of past climate
147 variability.

148 First, we describe MAIDEN and VS-Lite in Sect. 2.1, as well as the TRW
149 data network (Sect. 2.2) and climate data (Sect. 2.3) used in this study.

150 The calibration (Sect. 2.4) and verification (2.5) procedure of both models
151 is then presented. The models are calibrated and applied to the PAGES2k
152 TRW database in Sect. 3.1. We provide explanations on the performance of
153 the models in Sect. 3.2. The ability of MAIDEN and VS-Lite to reproduce the
154 climate signal in tree-rings is then evaluated in Sect. 3.3 and, finally, the impli-
155 cations of including atmospheric CO₂ concentration as an input of MAIDEN
156 are assessed in Sect. 3.4.

157 **2 Material and Methods**

158 **2.1 Tree-growth models**

159 *2.1.1 MAIDEN*

160 MAIDEN (Misson, 2004; Gea-Izquierdo et al., 2015; Gennaretti et al., 2017)
161 is a complex tree-growth model that explicitly includes biological processes
162 (photosynthesis and carbon allocation to different tree compartments) to sim-
163 ulate, among other outputs, the annual quantity of carbon allocated to the
164 stem. This key variable is hereafter referred to as Dstem, in grams of carbon
165 per square meter of stand per year. In this study, Dstem is assumed to be pro-
166 portional to tree-ring growth so as to compare it with TRW observations. The
167 model runs on a daily basis with maximum and minimum air temperature,
168 cumulative precipitation and atmospheric CO₂ concentration as inputs.

169 In this study, we use a combined version of the model from Gea-Izquierdo
170 et al. (2015) (initially developed for Mediterranean forests; hereafter GI2015)
171 and Gennaretti et al. (2017) (initially developed for boreal tree species; here-
172 after Ge2017) developed by Fabio Gennaretti (unpublished) that gives the
173 possibility to switch between those two versions. The versions from GI2015
174 and Ge2017 only differ in some mechanistic rules used in the photosynthetic
175 and allocation modules, but they are identical otherwise. The structure of
176 the MAIDEN model is provided online ([https://figshare.com/articles/
177 MAIDEN_ecophysiological_forest_model/5446435/1](https://figshare.com/articles/MAIDEN_ecophysiological_forest_model/5446435/1), last access: 16 May
178 2020) and its modules are available upon request.

179 The model includes constants to describe the conditions at the tree-ring
180 observations site and the climate station (Table S1). As in Rezsöhazy et al.
181 (2020), the constants are derived from observations. However, slope and as-
182 pect constants are set to zero, as we do not have the field knowledge needed to
183 extract the information from a Digital Elevation Model. MAIDEN includes
184 a four-layer soil module (1-15cm; 15-30cm; 30-65cm; 65-100cm) for which
185 we have to provide the main characteristics (clay and sand fractions; Ta-
186 ble S1). The soil characteristics are obtained from the Harmonized World
187 Soil Database (hereafter HWSD) v1.2 at a 30 arc-second spatial resolution
188 (FAO/IIASA/ISRIC/ISSCAS/JRC, 2012), as in Rezsöhazy et al. (2020).

189 *2.1.2 VS-Lite*

190 The Vaganov-Shashkin Lite model (Tolwinski-Ward et al., 2011) is a simple
191 tree-growth model that simulates a unitless annual tree-growth increment
192 based on latitude, monthly cumulative precipitation and average temperature
193 of the study site as inputs. It is based on the limiting factors principle
194 (temperature and soil moisture) and on the use of threshold growth response
195 functions. VS-Lite is derived from the full process-based Vaganov-Shashkin
196 model (Vaganov et al., 2006) that has been developed to explicitly quantify
197 the influence of climate and environmental variables on tree-ring formation.
198 While the full model is a two-block model, i.e. a block with cell growth, di-
199 vision and multiplication in the cambium and a growth block based on the
200 limiting factor principle, the Lite version just uses the second block.

201 *2.2 PAGES2k tree-ring width data*

202 The PAGES2k working group aims to reconstruct the climate of the last two
203 millennia based on proxy records (PAGES 2k Consortium, 2017). Their com-
204 munity database contains 692 temperature-sensitive proxy records from differ-
205 ent archives (trees, ice, sediment, coral, speleothems, documentary evidence,
206 and other archives), among which 354 TRW time series are of interest for our
207 work (PAGES 2k Consortium, 2017). We were able to retrieve the species in-
208 formation needed to run MAIDEN at 307 sites. Time series ending before 1979
209 were excluded to allow for a long enough calibration period (at least 30 years
210 starting from 1950, Sect. 2.4), leaving 302 TRW time series for our analysis
211 (Fig. 1). The resulting TRW network covers a large range of environmental
212 conditions and tree species (evergreen and deciduous), but is mostly located
213 in the Northern Hemisphere, specifically in North America and Asia. As a
214 consequence, the TRW network is dominated by cold and dry sites (Fig. S1).
215 The tree-ring proxy records in the PAGES2k database have been specifically
216 selected for their local sensitivity to temperature (PAGES 2k Consortium,
217 2017). However, correlations with other environmental variables can be signif-
218 icant as well, for example with precipitation, and a gradient of environmental
219 sensitivity is thus obtained (water limited sites, temperature limited sites or
220 unclear limiting factor). This can be illustrated by the comparison of the cor-
221 relations of TRW observations with annual cumulative precipitation against
222 the correlations with mean annual temperature over 1901-2000 (Fig. S2). A
223 wide range of values in the correlations is observed with both variables, with
224 the mean being slightly higher for temperature (0.07 mean correlation, com-
225 pared to 0.05 for precipitation). TRW data are available online (PAGES 2k
226 Consortium, 2017).

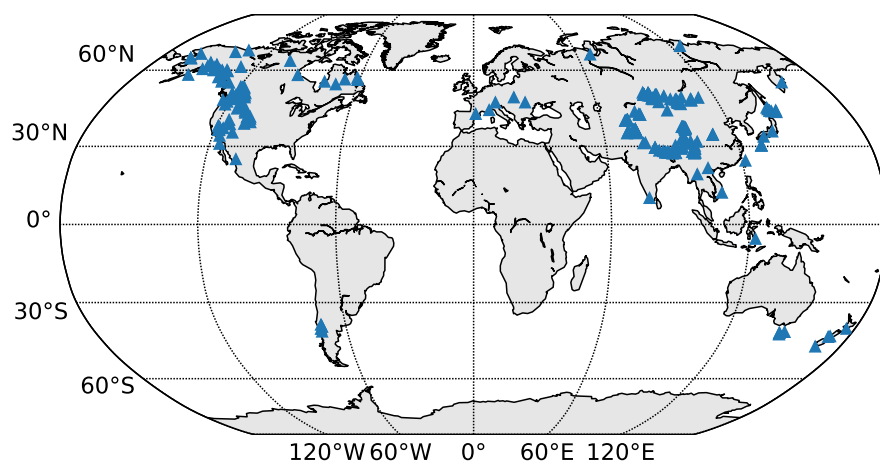


Fig. 1 PAGES2k (PAGES 2k Consortium, 2017) tree-ring width sites used in this study (302 sites). Background map from Hunter (2007).

2.3 Climate data

Daily climatic inputs are needed to run MAIDEN (Sect. 2.1.1) while VS-Lite needs monthly climate inputs (Sect. 2.1.2). In this study, we use the *Global Meteorological Forcing Dataset for land surface modelling (v2)* (<http://hydrology.princeton.edu/data.php>, last access: 13 March 2020; Sheffield et al., 2006) at 0.5° resolution over the 1901-1949 and 1950-2000 time periods. Daily maximum and minimum temperature and daily cumulative precipitation were extracted for MAIDEN from the grid cell closest to each individual site. Daily mean temperature and cumulative precipitation were averaged and summed, respectively, for VS-Lite at a monthly time step. Annual atmospheric CO₂ concentration data are from Sato and Schmidt (<https://data.giss.nasa.gov/modelforce/ghgases/>, last access: 6 January 2020) and were linearly interpolated at a daily time step. Note that for the Southern Hemisphere climate data start in July instead of January to match the seasonality of tree-growth.

2.4 Calibration

2.4.1 MAIDEN

A protocol has been developed in Rezsöhazy et al. (2020) to calibrate MAIDEN in a systematic and automatic way following a Bayesian procedure with Markov Chain Monte Carlo sampling using the DREAMzs algorithm (Hartig et al., 2019). Because we are working with the two versions of MAIDEN here (Gea-Izquierdo et al., 2015; Gennaretti et al., 2017), the procedure has been adapted

249 to the version from Gea-Izquierdo et al. (2015), that was not used in Rezsö-
250 hazy et al. (2020). The Bayesian procedure allows for calibration of the most
251 sensitive parameters of the model. This includes parameters influencing the
252 simulated stand growth primary production or GPP (6 parameters in the
253 Ge2017 version and 5 parameters in the GI2015 version) and parameters in-
254 fluencing the simulated daily quantity of carbon allocated to different tree
255 compartments (12 parameters in the Ge2017 version and 13 parameters in
256 the GI2015 version). Those parameters are referenced hereafter as photosyn-
257 thesis and carbon allocation parameters, respectively. The calibration starts
258 from prior distributions, assumed to be uniform over an acceptable range, to
259 produce posteriors for each of the 18 calibrated parameters. It is based on
260 the comparison between the normalized (i.e. with a null mean and a standard
261 deviation of 1) simulated annual quantity of carbon allocated to the stem or
262 Dstem and normalized observed TRW time series. Tables S2 and S3 give the
263 definition of each calibrated parameter for both versions. The ranges of the
264 parameters are available for both versions in Tables S4 and S5.

265 Ideally, photosynthesis parameters should be calibrated by comparing sim-
266 ulated against observed GPP instead of simulated Dstem against observed
267 TRW and prior ranges would have been more informative for each species
268 or biome (Misson, 2004; Danis et al., 2012; Gea-Izquierdo et al., 2015, 2017;
269 Gennaretti et al., 2017; Lavergne et al., 2017). However, this is not possible
270 here as the information is lacking for the majority of sites. Furthermore, the
271 tree-growth index simulated by MAIDEN, which is derived from the annual
272 quantity of carbon allocated to the stem, is not directly comparable to TRW
273 without standardization. We are thus unable to both calibrate the variance and
274 evaluate the error variance of tree-growth (Rezsöhazy et al., 2020). Information
275 is thus missing to guide the Bayesian calibration towards a biologically plausi-
276 ble set of parameters. For example, we miss information to properly constrain
277 phenology. Consequently, the selection of parameters for our simulations has
278 been slightly updated compared to Rezsöhazy et al. (2020). The set of photo-
279 synthesis parameters with the highest posterior (Maximum *a posteriori* value
280 or MAP; Hartig et al., 2019) is selected as in Rezsöhazy et al. (2020). The car-
281 bon allocation parameters are then calibrated as in Rezsöhazy et al. (2020).
282 In addition, after the calibration procedure, the model is iteratively run over
283 the top 10% carbon allocation parameters. The photosynthesis parameters are
284 fixed at their calibrated values. To avoid unrealistic growth period lengths, a
285 parameter set which simulates a growth period of less than 20 days for each
286 year of the calibration period (hereafter, phenological criterion) is excluded.
287 At the end of the iterations, we keep the set of parameters with the highest
288 likelihood. Note that if none of the parameter sets meet the phenological cri-
289 terion, the MAIDEN calibration is considered as non-valid for this site with
290 the forcing used.

291 MAIDEN was calibrated at the TRW sites with at least 30 TRW observa-
292 tions available over the 1950-2000 period, using the climate data described in
293 Sect. 2.3. For simplicity, the calibration period will be referred to as 1950-2000.

2.4.2 VS-Lite

The Bayesian approach proposed in Tolwinski-Ward et al. (2013) was used to calibrate the four VS-Lite parameters linked to the growth response (lower and upper temperature and soil moisture thresholds of the model; T_1 and T_2 , and M_1 and M_2 , respectively, in Tolwinski-Ward et al., 2011). This Bayesian approach is based on a standard Markov Chain Monte Carlo method to sample the posterior distribution, i.e., a Metropolis-Hastings algorithm embedded within a Gibbs sampler. Default values were given to the other parameters (six soil moisture parameters and two integration window parameters) as provided in the standard version of the model code (<https://www.ncei.noaa.gov/pub/data/paleo/softlib/vs-lite/>, last access: 16 March 2021).

VS-Lite was optimized at the 302 TRW sites over the same time period as MAIDEN and using the climate dataset described in Sect. 2.3.

2.5 Verification

Both models were tested over the 1901-1949 time period, with the same climate data as described in Sect. 2.3. Models were run over the verification period using the parameters calibrated over the 1950-2000 time period as in Sect. 2.4. Pearson correlation coefficients and their corresponding confidence levels were calculated at each site between simulated tree-ring indexes from MAIDEN or VS-Lite and observed TRW on both the calibration and the verification time periods.

3 Results

Section 3.1 assesses and compares the general performance of both VS-Lite and MAIDEN models with respect to calibration (Sect. 2.4) and independent verification (Sect. 2.5), in order to determine the sites with the best performance. Section 3.2 explains the performance of both models, by focusing on its relationship with different environmental characteristics, such as climate and tree leaf traits. Section 3.3 evaluates the ability of both PSMs to reproduce the climate signal recorded in tree-rings, and then their potential for paleoclimate data assimilation based reconstructions. Finally, Section 3.4 assesses the effect of CO_2 concentration in the MAIDEN model with a sensitivity analysis.

3.1 Applying MAIDEN and VS-Lite to the PAGES2k TRW sites

Substantial challenges arose in the calibration of MAIDEN. In particular, at some sites, we were unable to properly set phenology due to the lack of information available for calibration (Sect. 2.4.1). From all 302 calibration experiments (Sect. 2.4.1), 113 sites for Ge2017 and 142 sites for GI2015 were excluded based on the phenological criterion (Sect. 2.4.1). The remaining sites (189 sites for

331 Ge2017 and 160 sites for GI2015) will be referred to as MAIDEN selected sites.
332 All the analyses for MAIDEN are performed on these selected sites. From all
333 calibration (Sect. 2.4.1) and verification (Sect. 2.5) experiments for both ver-
334 sions (Gea-Izquierdo et al., 2015; Gennaretti et al., 2017) of MAIDEN (Figs.
335 S3 – S6), we consider a site as well-fitted only if the following conditions are
336 fulfilled, whatever the model version used: (i) a significant (at the 95% con-
337 fidence level) calibration (1950-2000) and verification (1901-1949) correlation
338 ≥ 0.3 ; (ii) a growth period length of at least 20 days for each year of the cali-
339 bration (Sect. 2.4.1) and verification period. If conditions are fulfilled for both
340 versions, the version leading to the highest verification correlation at the site
341 is kept. Based on these criteria, we retained 64 well-fitted sites (Fig. 2a).

342 For VS-Lite (Sect. 2.4.2 and 2.5; Figs. S7 and S8), the condition for retain-
343 ing a site is also to have a significant (at the 95% confidence level) calibration
344 (1950-2000) and verification (1901-1949) correlation ≥ 0.3 . As for MAIDEN,
345 VS-Lite simulated time series were checked for consistency as correlation is
346 not able to account for all artefacts in simulated chronologies. Two sites were
347 considered as invalid since estimated tree-growth indexes were found constant
348 (no growth) for more than 10 successive years. Based on these criteria, we
349 retained 63 well-fitted sites (Fig. 2b).

350 Considering the loss of correlation from calibration to verification, VS-Lite
351 appears more stable than MAIDEN (Fig. 3, see Fig. S9 for by-site correlations).
352 Calibrating MAIDEN at the global scale without overfitting is indeed a chal-
353 lenge. The mean calibration and mean verification correlations for MAIDEN
354 are 0.68 (with a standard deviation of 0.10) and 0.43 (0.10) respectively, and
355 0.49 (0.14) and 0.43 (0.11) for VS-Lite. 18 well-fitted sites are in common
356 between VS-Lite and MAIDEN (Fig. 4). On average, verification correlations
357 are 0.47 for MAIDEN and 0.48 for VS-Lite with a standard deviation of 0.10
358 and 0.14 respectively. MAIDEN and VS-Lite are skillful at a similar num-
359 ber of mostly different sites, spread all over the globe. The reasons behind
360 their performance are consequently also different and will be addressed in the
361 next section. However, at the common sites, their respective performances are
362 equivalent.

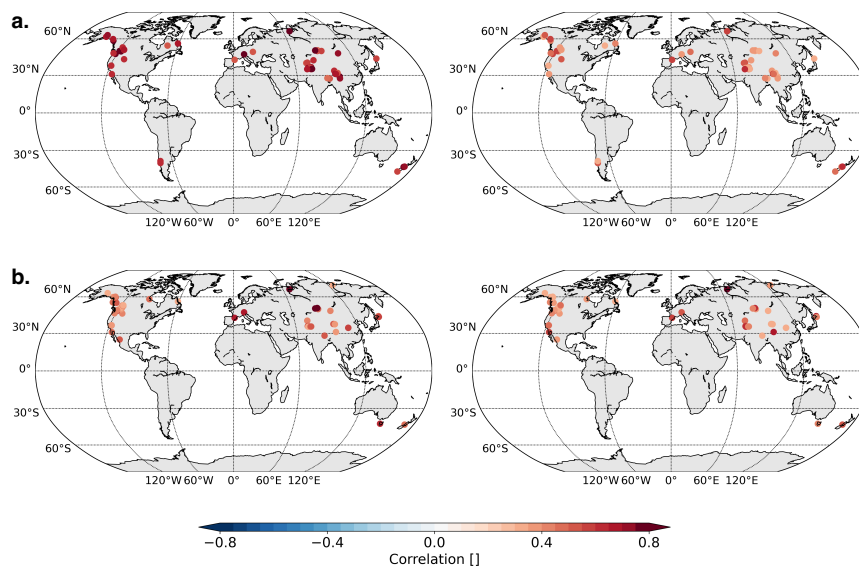


Fig. 2 (a) MAIDEN (64 sites) and (b) VS-Lite (63 sites) calibration (left) and verification (right) correlations for well-fitted sites (Sect. 3.1). All correlations are significant at the 95% confidence level. Background maps from Hunter (2007).

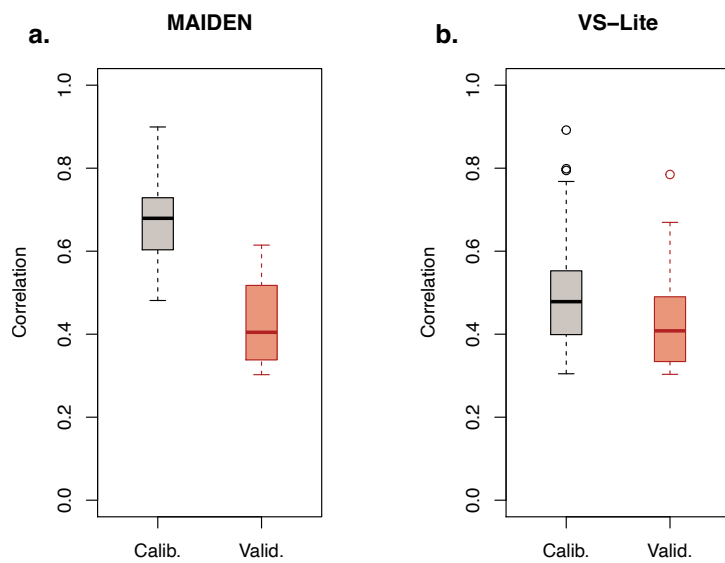


Fig. 3 (a) MAIDEN (64 sites) and (b) VS-Lite (63 sites) calibration (1950-2000) and verification (1901-1949) correlations (all significant at the 95% confidence level) boxplots for well-fitted sites (Sect. 3.1).

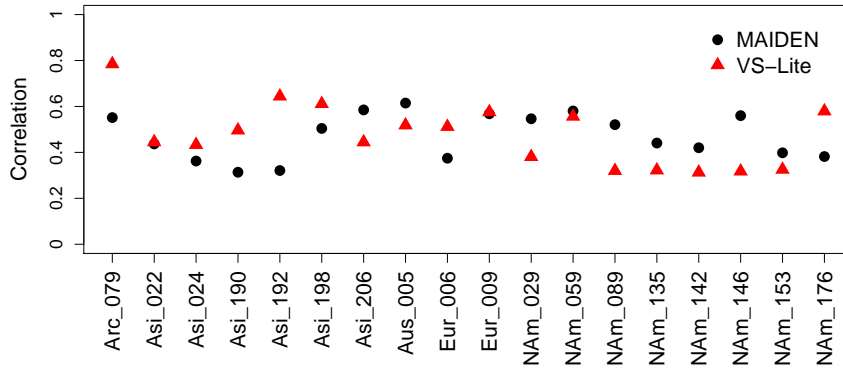


Fig. 4 MAIDEN and VS-Lite verification (1901-1949) correlations (all significant at the 95% confidence level) for common well-fitted sites (Sect. 3.1) (18 sites, with names from the PAGES2k database: *NAm* for North American sites; *Asi* for Asian sites; *Eur* for European sites; *Arc* for Arctic sites; *Aus* for Australian, Tasmanian or New Zealand sites; *SAm* for South American sites).

363 3.2 Explaining the performance of VS-Lite and MAIDEN

364 In this section, we want to understand the underlying factors driving the per-
 365 formance of both models. We focus on two site characteristics: tree leaf traits
 366 and climate. The relationship between models performance and altitude, lati-
 367 tude or calibration period length (ranging from 30 to 51 years) was also checked
 368 but none of these variables were found to be a significant driver of models skill.
 369 We are here considering all calibrated sites (Sect. 2.4), irrespective of whether
 370 they were identified as well-fitted in the previous section or not.

371 Verification correlations as a function of tree leaf traits (deciduous or ev-
 372 ergreen) are shown on Fig. 5 for both versions of MAIDEN and for VS-Lite.
 373 VS-Lite performance (Fig. 5c) does not seem to be influenced by leaf trait, with
 374 an average correlation of 0.184 and 0.221 for deciduous and evergreen trees
 375 respectively. 13 sites out of 63 well-fitted sites are deciduous which is compar-
 376 able to the proportion of deciduous sites in the PAGES2k TRW database
 377 (64 deciduous out of 302 sites, i.e. around 20%). For MAIDEN (Fig. 5a and
 378 b), verification correlations are also very close on average for deciduous (0.073
 379 for GI2015 and 0.101 for Ge2017) and evergreen trees (0.087 for GI2015 and
 380 0.113 for Ge2017). However, there is a low proportion of deciduous trees for
 381 Ge2017 (Fig. 5b) that passes the phenological criterion for the calibration de-
 382 scribed in Sect. 2.4.1 (9 out of 64 sites) compared to evergreen trees (180 out
 383 of 238 sites). Conversely, this proportion is far higher for GI2015 (36 sites out
 384 of 64; Fig. 5a) and comparable to evergreen trees (124 sites out of 238). Be-
 385 sides, seven sites out of 64 well-fitted sites are deciduous which is less than the
 386 proportion of deciduous sites in the PAGES2k TRW database (64 out of 302

387 sites). Only one deciduous well-fitted site is simulated by Ge2017, and six by
388 GI2015. A possible reason is that only the version from Gea-Izquierdo et al.
389 (2015) has already been applied to deciduous trees sites (*Quercus Pyrenaica*;
390 Gea-Izquierdo et al., 2017). Consequently, we were able to use the initializa-
391 tion parameters already applied to deciduous trees in this version solely. The
392 version from Gennaretti et al. (2017) has never been specifically calibrated
393 for deciduous trees and some initialization parameters are likely not adapted
394 in that case. This exemplifies the fact that the calibration and initialization
395 of MAIDEN are probably the main obstacles for a better performance of the
396 model at the global scale.

397 To study the influence of climate on the performance of both models, we
398 focus on different climate indicators: cumulative October to September pre-
399 cipitation, annual mean temperature and mean July-August-September tem-
400 perature. In general, correlations of climate indicators with verification scores
401 at all sites are low and not significant for both VS-Lite and MAIDEN (Table
402 S6). This means that the performance of both models does not depend primar-
403 ily on the mean climate at a site. Another hypothesis to test is whether the
404 models perform better for sites where tree-ring growth is strongly controlled
405 by climate. To this end, we compare the correlations between climate vari-
406 ables and observed TRW to the verification correlations (Table 1). Since none
407 of the correlations in Table 1 are significant (p-value < 0.05) for MAIDEN,
408 its performance does not rely significantly on tree-growth correlation with
409 climate. On the contrary, VS-Lite performance shows a higher dependency
410 on tree-growth correlation with climate, especially temperature (Table 1). In-
411 deed, all correlations between the tree-growth relationship with climate and
412 verification scores for VS-Lite are significant and particularly high for annual
413 (0.467) and July-August-September (0.506) temperature. We obtain the same
414 result for VS-Lite when the analysis is restricted to the MAIDEN selected
415 sites (Sect. 2.4.1) (Table S7). This dependence of VS-Lite performance to the
416 presence of a strong climate driver of tree-growth is consistent with what has
417 been highlighted in Breitenmoser et al. (2014). It is likely due to the struc-
418 ture of VS-Lite on itself (Sect. 2.1.2), as tree-growth directly depends on the
419 identified limiting climatic factor (temperature or soil moisture) at the site
420 in the model. VS-Lite tends to be better where tree-growth is predominantly
421 driven by climate, which can be limiting for its application in many regions of
422 the world away from the treeline environments (for example high-altitude or
423 high-latitude environments), often not considered for paleoclimate reconstruc-
424 tion (Breitenmoser et al., 2014; Babst et al., 2018). Conversely, in MAIDEN,
425 multiple biological processes shape the links that exist between climate and
426 tree-growth. This potentially brings a better suitability of MAIDEN to work in
427 a larger range of environments than VS-Lite, where the relationship between
428 climate and tree-growth is more complex.

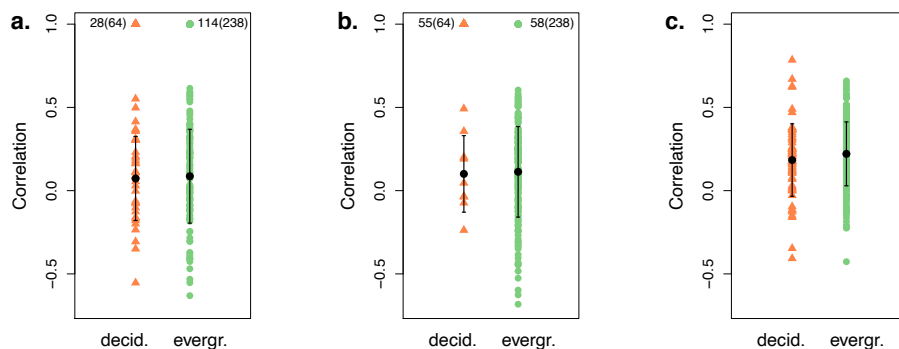


Fig. 5 Verification correlations, mean and standard deviation by tree types (deciduous or evergreen) for the MAIDEN version of GI2015 (a) and Ge2017 (b), for selected sites (160 sites for GI2015 and 189 for Ge2017, Sect. 2.4.1; others have been put to 1; the number of sites that have been put to 1 is indicated by category with the total number of sites in each category in brackets) and VS-Lite, for all 302 sites (c).

Table 1 Pearson correlations between correlations of observed TRW with different climate indicators and MAIDEN or VS-Lite verification correlations (1901-1949). O-S stands for the year starting from October (previous year) to September (current year); P for precipitation; JAS for July-August-September; T for temperature. Asterisks stand for significant correlations (p -value < 0.05). The difference in the number of sites on which correlations are computed is due to the phenological criterion that has been applied to MAIDEN calibrated sites (see Sect. 2.4.1 for more details).

Model (version)	Correlation
Correlations between observed TRW and O-S P correlation and verification correlation	
MAIDEN (Ge2017; 189 sites)	0.114
MAIDEN (GI2015; 160 sites)	0.155
VS-Lite (302 sites)	0.149*
Correlations between observed TRW and annual T correlation and verification correlation	
MAIDEN (Ge2017; 189 sites)	0.074
MAIDEN (GI2015; 160 sites)	0.059
VS-Lite (302 sites)	0.467*
Correlations between observed TRW and JAS T correlation and verification correlation	
MAIDEN (Ge2017; 189 sites)	-0.039
MAIDEN (GI2015; 160 sites)	-0.097
VS-Lite (302 sites)	0.506*

429 3.3 Assessing the ability of MAIDEN and VS-Lite to reproduce climate
430 relationship with tree-growth

431 One of the ultimate purposes of PSMs like VS-Lite and MAIDEN is to be
432 used to reconstruct past climates, for example by including them in a data

433 assimilation procedure (Evans et al., 2013; Dee et al., 2016). Therefore, we
434 have to assess if these models are able to reproduce well the climate signal
435 recorded in TRW. In the previous section, we established if the models ability
436 to reproduce tree-growth depends on the presence of a strong climate signal
437 recorded in the tree rings. In this section, we want to evaluate if the simulated
438 climate signal, whatever its predominance, is consistent with its recording by
439 tree-ring indexes. This is based on the comparison of the correlations of dif-
440 ferent climate indicators with tree-growth in simulations and in observations:
441 firstly, by means of scatterplots (Figs. 6, 7 and 8) and secondly, by means of
442 correlations (Table 2).

443 For MAIDEN (Figs. 6 and 7), over- and underestimations of the climate
444 dependencies of tree-growth are more balanced than for VS-Lite (Fig. 8) as
445 the dots in the scatterplots tend to spread more equally around and are closer
446 to the 1:1 line, particularly for temperature. Conversely, the scatterplots of
447 VS-Lite (Fig. 8) show a stronger overestimation of the climate dependency of
448 tree-growth at most sites, as most of the dots are far above the diagonal. This
449 bias is particularly large for temperature. Indeed, for VS-Lite, the correlation
450 for mean annual temperature is overestimated by more than 0.4 at 43% of
451 the sites (12% for GI2015 and 18% for Ge2017), at 47% of the sites for mean
452 July-August-September temperature (7% for GI2015 and 13% for Ge2017),
453 and at 28% of the sites for October-September cumulative precipitation (17%
454 for GI2015 and 12% for Ge2017). The same conclusion is still valid for VS-Lite
455 when we restrict the analysis to the MAIDEN selected sites (Sect. 2.4.1) (Figs.
456 S10-S15). This overestimation of the climate signal enhanced by the model is
457 a crucial feature to consider when using such PSMs in paleoclimatology, as
458 it can lead to biased climate reconstruction. Again, the structure of VS-Lite
459 is likely responsible for the overestimation of the climate influence on tree-
460 growth as tree-growth is not driven by any other internal or external drivers
461 than limiting climatic factors. The very high correlations ($r > 0.7$) between the
462 VS-lite simulations and basic climate indicators on Fig. 8 at many sites indi-
463 cate the simplicity of the climate dependence of tree-growth in this PSM. In
464 MAIDEN, many biological processes are in play to frame the climate depen-
465 dence of tree-growth. MAIDEN uses different functional rules specific to the
466 ongoing phenological phase to allocate at a daily time step the available carbon
467 from photosynthesis and stored non-structural carbohydrates to different tree
468 compartments. The functional rules directly depend on climate factors, such
469 as growing degree days, soil water content or temperature, and are specific to
470 the phenological phase. Simultaneously, the daily photosynthesis is simulated
471 following the biochemical model of Farquhar et al. (1980) and dynamically in-
472 teracts with the allocation module. The combination and interaction of these
473 processes may smooth out the direct climate signal on tree-ring growth.

474 Correlations between observed and simulated (MAIDEN or VS-Lite) tree-
475 growth dependency on climate at all sites are generally low (ranging from
476 0.053 to 0.515), particularly for temperature, even if mostly significant (Table
477 2). The correlations for VS-Lite when we restrict the analysis to the MAIDEN
478 selected sites (Sect. 2.4.1) are in Table S8 and are similar to the results for

479 all 302 sites. In other words, when considering all sites, both models have low
 480 skill in reproducing correctly the actual climate signal observed in tree-rings.
 481 However the well-fitted sites (Sect. 3.1) have better correlations, ranging from
 482 0.648 (annual temperature) to 0.759 (July-August-September temperature)
 483 for MAIDEN and 0.678 (annual temperature) to 0.837 (October-September
 484 precipitation) for VS-Lite. Both models are thus able to accurately mimic
 485 the climate signal in tree-ring observations if the sites are carefully selected
 486 (Sect. 3.1). When focusing on the common well-fitted sites between VS-Lite
 487 and MAIDEN, VS-Lite is slightly better at reproducing climate, specifically
 488 for annual temperature (0.608 correlation for MAIDEN and 0.772 for VS-Lite)
 489 and precipitation (0.747 for MAIDEN and 0.886 for VS-Lite).

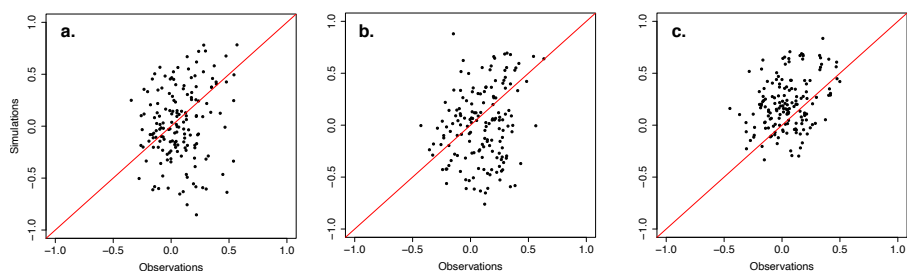


Fig. 6 Correlations between mean annual temperature (a), mean July-August-September temperature (b), October-September cumulative precipitation (c) and MAIDEN (GI2015) Dstem simulations as a function of correlations between the same climate indicators and TRW observations for selected sites (160 out of 302 sites; Sect. 2.4.1) over the 1901-1949 verification period.

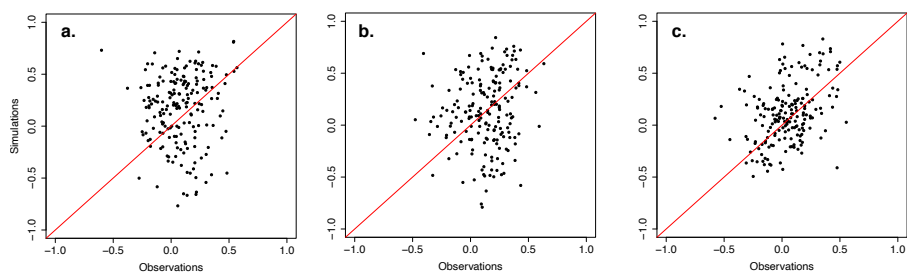


Fig. 7 Correlations between mean annual temperature (a), mean July-August-September temperature (b), October-September cumulative precipitation (c) and MAIDEN (Ge2017) Dstem simulations as a function of correlations between the same climate indicators and TRW observations for selected sites (189 out of 302 sites; Sect. 2.4.1) over the 1901-1949 verification period.

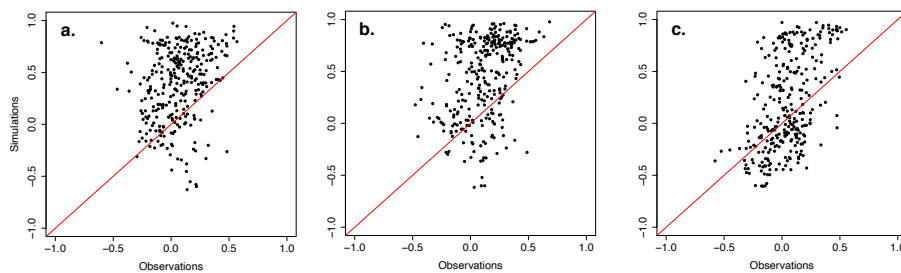


Fig. 8 Correlations between mean annual temperature (a), mean July-August-September temperature (middle), October-September cumulative precipitation (b) and VS-Lite tree-ring index simulations as a function of correlations between the same climate indicators and TRW observations for all sites (302) over the 1901-1949 verification period.

Table 2 Pearson correlations of correlations between different climate indicators and tree-ring width observations with correlations between the same climate indicators and MAIDEN or VS-Lite tree-growth simulations (1901-1949 verification period). O-S stands for the year starting from October (previous year) to September (current year); P for precipitation; JAS for July-August-September; T for temperature; TRindex for tree-ring index. Asterisks stand for significant correlations (p -value < 0.05). The difference in the number of sites on which correlations are computed is due to the phenological criterion that has been applied to MAIDEN calibrated sites (see Sect. 2.4.1 for more details).

Model (version)	Correlation
Correlations between observed TRW and O-S P correlation and simulated TRindex and O-S P correlation	
MAIDEN (Ge2017; 189 sites)	0.388*
MAIDEN (GI2015; 160 sites)	0.322*
VS-Lite (302 sites)	0.515*
MAIDEN (well-fitted sites only)	0.694*
VS-Lite (well-fitted sites only)	0.837*
MAIDEN (common well-fitted sites only)	0.747*
VS-Lite (common well-fitted sites only)	0.886*
Correlations between observed TRW and annual T correlation and simulated TRindex and annual T correlation	
MAIDEN (Ge2017; 189 sites)	0.053
MAIDEN (GI2015; 160 sites)	0.171*
VS-Lite (302 sites)	0.241*
MAIDEN (well-fitted sites only)	0.648*
VS-Lite (well-fitted sites only)	0.678*
MAIDEN (common well-fitted sites only)	0.608*
VS-Lite (common well-fitted sites only)	0.772*
Correlations between observed TRW and JAS T correlation and simulated TRindex and JAS T correlation	
MAIDEN (Ge2017; 189 sites)	0.130
MAIDEN (GI2015; 160 sites)	0.216*
VS-Lite (302 sites)	0.338*
MAIDEN (well-fitted sites only)	0.759*
VS-Lite (well-fitted sites only)	0.704*
MAIDEN (common well-fitted sites only)	0.739*
VS-Lite (common well-fitted sites only)	0.787*

490 3.4 Sensitivity analysis of MAIDEN to atmospheric CO₂ concentration

491 In this section, we perform a sensitivity analysis of the MAIDEN model to
492 atmospheric CO₂ concentration. The CO₂ concentration is a key driver of the
493 forest carbon fluxes but its actual effects are still difficult to consider and
494 evaluate in dendroecological studies (Körner et al., 2005; Silva et al., 2010;
495 Peñuelas et al., 2011; Lévesque et al., 2014; Van Der Sleen et al., 2015; Girardin
496 et al., 2016; Hararuk et al., 2019; Giguère-Croteau et al., 2019; Marchand et al.,
497 2020). Yet, the CO₂ concentration has increased by 30% over the last 50 years
498 and might increase up to 1000 ppm at the 2100 horizon (RCP 8.5; Myhre
499 et al., 2013) relative to the current 414.49 ppm (December 2020, [https://
500 www.esrl.noaa.gov/gmd/ccgg/trends/global.html](https://www.esrl.noaa.gov/gmd/ccgg/trends/global.html), last access: 19 March
501 2021), which will have an impact on the forest carbon fluxes. This effect should
502 be taken into account in dendroecological analysis (Babst et al., 2018). In
503 MAIDEN, the CO₂ influences the forest carbon fluxes through the coupled
504 modelling of photosynthesis and stomatal conductance (Farquhar et al., 1980;
505 Leuning, 1995) with environmental dependencies related to temperature and
506 soil water content (Gea-Izquierdo et al., 2015; Gennaretti et al., 2017), and the
507 feedbacks between the coupled photosynthesis-stomatal conductance system
508 and the carbon allocation.

509 Here, we evaluate the influence of the inclusion of the CO₂ concentration
510 increase in MAIDEN by comparing its performance in the standard configu-
511 ration with a sensitivity experiment in which the CO₂ concentration is kept
512 constant, for the 64 well-fitted sites (Sect. 3.1), with parameters calibrated
513 based on the CO₂ increasing scenario. The CO₂ is fixed at its 1st January
514 1980 value for the Northern Hemisphere (339 ppm), and at its 1st July 1980
515 value for the Southern Hemisphere (340 ppm).

516 At each site, we computed the difference between normalized MAIDEN
517 tree-ring growth simulations and normalized TRW observations from 1990 with
518 increasing CO₂ and constant CO₂. We performed our analysis on the 60 sites
519 out of 64 well-fitted sites that end at least in 1990. Note that both simulations
520 were normalized over 1950-2000 based on the mean and standard deviation of
521 the original simulation, i.e. with increasing CO₂, over the same time period.
522 The density distributions of the difference for both experiments are shown
523 on Fig. 9a. The Pearson's Chi-squared test indicates a significant difference
524 between the two experiments distributions (p-value < 0.05). The mean for both
525 experiments are -0.209 and 0.182 for the constant CO₂ and increasing CO₂
526 experiment, respectively. In other words, while not taking into account CO₂
527 tends to underestimate the actual tree-growth on average, taking into account
528 the increase of CO₂ in MAIDEN leads to overestimate it. Ecophysiological
529 models are indeed known to overestimate the actual effect of CO₂ (Peñuelas
530 et al., 2011; Gea-Izquierdo et al., 2017). However, the CO₂ concentration has
531 certainly an impact on the tree carbon assimilation (Marchand et al., 2020)
532 that should be properly considered to avoid potential biases in climate and
533 growth trend reconstructions derived from tree-ring data. This impact can be
534 taken into account by ecophysiological models such as MAIDEN, but potential

535 overestimations must be carefully envisaged due to the generic default of such
536 models.

537 The trend of simulated and observed tree-growth was also computed and
538 compared at each of the 60 sites. It corresponds to the coefficient of regression
539 of the normalized tree-growth simulations or observations from 1970 up to 1990
540 at least, versus the years. The simulated trend by MAIDEN may reproduce
541 the generally positive trend that is observed from 1970 in TRW time series
542 (Fig. 9b) in correlation with the increasing CO₂ concentrations.

543 Consequently, our results show that the growth trends simulated by MAIDEN
544 are significantly influenced by the CO₂ increase and that MAIDEN simulated
545 tree-growth is closer to the observed TRW when including the CO₂ concentra-
546 tion increase. This limited analysis is not sufficient to draw conclusions
547 regarding CO₂ fertilization in trees but it highlights a potential CO₂ effect
548 based on a model that takes into account a commonly used biochemical for-
549 mulation of photosynthesis (Farquhar et al., 1980). Including the effect of CO₂
550 in a mechanistic model like MAIDEN is a potential advantage over statistical
551 and simple process-based models such as VS-Lite that are not able to account
552 for these processes strongly influencing the forest carbon fluxes. However, be-
553 cause of the remaining uncertainties on the associated processes, an improved
554 representation of the effect of CO₂ in process-based dendroecological models
555 is needed to analyse past and future growth trends and variability.

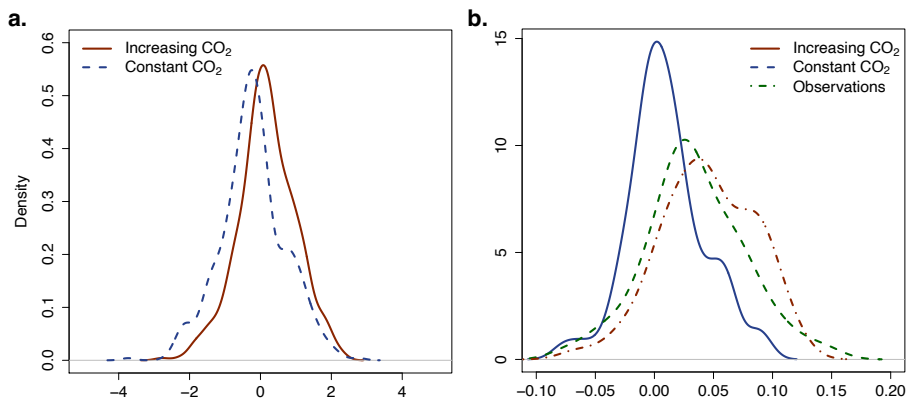


Fig. 9 Density distributions of (a) the difference between normalized tree-ring index simulations by MAIDEN and observed tree-ring width from 1990 with increasing CO₂ concentration (in red, i.e. the original configuration), and constant CO₂ concentration (in blue); (b) the trend from 1970 of normalized tree-ring index simulations by MAIDEN with increasing CO₂ concentration (in red, i.e. the original configuration) or with constant CO₂ concentration (in blue), and of normalized tree-ring width observations (in green); at 60 out of 64 well-fitted sites (Sect. 3.1).

4 Discussion and conclusions

In this paper, we have applied and compared two dendroclimatic process-based models of different complexity levels, VS-Lite and MAIDEN, using the global PAGES2k TRW database over the last century. We have evaluated their respective abilities and advantages to be used at the global scale as PSMs for paleoclimate data assimilation based reconstructions.

The models appear to be skillful for a similar number of mostly different sites (63 sites for VS-Lite and 64 sites for MAIDEN, 18 sites in common), spread over all continents. The performance of the models is comparable in terms of calibration and verification correlations. VS-Lite generally results in more stable correlations between the calibration and verification periods. When focusing on the factors that can drive the performance of both models, VS-Lite displays a strong correlation between its verification scores and tree-growth correlations with temperature, while MAIDEN does not. This means that VS-Lite tends to perform better at sites where observed tree-growth strongly correlates with temperature. In other words, the model's performance is improved in environments characterized by extreme temperatures. This feature hampers its application in many regions of the world away from the treeline, already rarely considered for paleoclimate reconstruction. In contrast, MAIDEN performance is less sensitive to the climate signal in TRW time series. We presume that MAIDEN performance is mainly limited by the lack of information needed to accurately calibrate and initialize the model at each specific site. As mentioned above, the information needed to calibrate MAIDEN is a key limitation of complex tree-growth models in general for use at a broader scale. This lack of data (for example, the observed Gross Primary Productivity data) also hinders a complete evaluation and identification of the factors driving the performance of MAIDEN.

At the sites where each model works well in terms of calibration and verification correlations, both VS-Lite and MAIDEN are on average able to successfully retrieve the climate signal in tree-rings. A careful selection of the tree-ring sites provides the opportunity to focus on the most robust simulated relationship between climate and tree-growth. However, VS-Lite appears to predominantly overestimate the observed dependence of tree-growth on climate, while there is no systematic bias for MAIDEN. The overestimation of the climate signal recorded in tree-rings has to be carefully taken into account when using such tree-growth models for data assimilation based reconstructions as it can result in biases. This is a clear disadvantage when using less complex dendroclimatic models, such as VS-Lite, in which the climate and tree-growth relationship is simplified.

Consequently, we may recommend using MAIDEN especially when the relationship between climate and tree-growth is complex with interacting limiting factors. VS-Lite would be a good candidate if tree-growth is mostly limited by only one climatic factor (e.g. summer temperature), although it may overestimate these climate dependences, particularly for temperature, leading to overconfident reconstructions. In this case, MAIDEN should produce more

601 plausible results. However, if not enough data are available to properly set
602 and calibrate MAIDEN (for example long daily climate data or soil charac-
603 teristics), VS-Lite should be preferred. As shown in Rezsöházy et al. (2020),
604 MAIDEN cannot be properly calibrated if used with short and low-replicated
605 TRW time series (periods shorter than 50 years).

606 It has also been shown in this study that the inclusion of atmospheric CO₂
607 concentration has a significant impact on the MAIDEN simulations. More
608 generally, MAIDEN appears as a potential good candidate to account for the
609 non-stationarity of the tree-growth-to-climate relationship linked to changing
610 CO₂ conditions in paleoclimate reconstructions. In particular, ecophysiological
611 models, such as MAIDEN, could be useful tools to solve the so-called diver-
612 gence problem in dendroclimatology (D'Arrigo et al., 2008). Conversely, from
613 a paleoclimate perspective, not taking into account changing CO₂ concentra-
614 tion when using PSMs for data assimilation based reconstructions could lead to
615 inaccurate climate reconstructions. More specifically, models such as VS-Lite
616 could wrongly assign a trend in TRW series due to CO₂ concentration changes
617 to the effect of rising temperatures. In turn, this will lead to an overestimation
618 of the climate sensitivity of tree-growth and thus to an overestimation of the
619 amplitude of past reconstructions. However, the impact of CO₂ concentration
620 on tree carbon assimilation in more complex ecophysiological models should
621 be evaluated carefully to properly take this process into account.

622 Consequently, future reconstructions and data assimilation could benefit
623 from the use of complex ecophysiological models such as MAIDEN. Despite
624 the obvious challenges that are associated with the calibration of such models,
625 their potential for improving the quality of the reconstructions makes their
626 complexity worthy. In particular, they widen the range of environments where
627 tree-ring observations can be used for dendroclimatic reconstructions, includ-
628 ing regions where the relationship between TRW and climate is more com-
629 plex. They also account for the potential non-stationarity of tree-growth, for
630 example due to increasing CO₂ concentration. Finally, they can prevent from
631 systematic bias in the reconstruction of the climate signal recorded in TRW
632 observations. Additionally, ecophysiological models like MAIDEN are contin-
633 uously benefiting from improvements made in ecophysiology, in particular in
634 the modelling of the links between climate and tree-growth through complex
635 biological processes. However, in order to optimally use these complex models,
636 we need to (1) have additional site knowledge to properly initialize the model
637 such as data on the root profile, (2) use additional observations to verify spe-
638 cific processes such as phenology and photosynthetic rates, and (3) verify that
639 the tree-ring chronologies are not affected by sampling biases that can dis-
640 tort the growth trends or are linked to non-climatic processes such as tree
641 ontogeny and demographic changes in the sampled stands (Duchesne et al.,
642 2019). Finally, to properly calibrate a complex model such as MAIDEN at
643 the global scale, multiple data information sources should be mixed in the
644 future. For example, tree phenology is hard to set with tree-ring data only.
645 The phenology of MAIDEN could be informed more efficiently using satel-
646 lite data (e.g. NDVI). On the other hand, simple dendroclimatic models like

647 VS-Lite, through their ease of use and calibration, coupled with a satisfying
648 performance in reproducing tree-growth, are also appealing candidates for pa-
649 leoclimate data assimilation based reconstructions. VS-Lite and MAIDEN thus
650 bring complementary assets for reconstructing past climates. The user must
651 select the model according to the goal of the study (temperature or hydrocli-
652 mate reconstruction), the data availability at the proxy site and the climate
653 dependence of the TRW observations (one or multiple climate drivers).

654 More generally, the simultaneous evaluation of tree-growth PSMs of dif-
655 ferent complexity is essential for any future paleoclimate data assimilation
656 exercises willing to use TRW proxy data and tree-ring PSMs at the global
657 scale. Such study helps to select the adequate PSM and identify the limita-
658 tions and the advantages of mechanistic modelling in a paleoclimate perspec-
659 tive compared to statistical methods. It is thus a necessary step to increase our
660 ability to robustly reconstruct past climates from tree-rings. In particular, our
661 work sheds light on how process-based dendroclimatic models can improve the
662 skill of reconstructions of past climate from tree-rings in comparison with the
663 commonly used linear reconstruction methods. We have shown that the mech-
664 anistic approach has great potential to enhance our understanding of the past
665 climate variability. Consequently, the next step will be to include such models
666 in a data assimilation procedure to reconstruct the climate of the last millen-
667 nium in regions where the models perform well. On this basis, we will be able
668 to fully evaluate how process-based dendroclimatic models can contribute to
669 the improvement of large-scale reconstructions of past climate variability and
670 justify the added complexity of the procedure compared to linear regressions.

671 **Acknowledgements** We gratefully thank François Klein and Marie Cavitte for their com-
672 ments on the manuscript. JR is F.R.S-FNRS Research Fellow, Belgium (grant no. 1.A841.18);
673 FG received funding by the Quebec Ministry of forests, wildlife and parcs (MFFP; contract
674 number 142332177-D); HG is research director at F.R.S.-FNRS, Belgium; JG is research
675 director at CNRS, France. This publication has received partial funding from Laboratory of
676 Excellence OT-Med (project ANR-11- LABEX-0061, A*MIDEX project 11-IDEX-0001-02).
677 Computational resources have been provided by the supercomputing facilities of the Uni-
678 versité catholique de Louvain (CISM/UCL) and the Consortium des Équipements de Calcul
679 Intensif en Fédération Wallonie Bruxelles (CÉCI) funded by the Fond de la Recherche Scien-
680 tifique de Belgique (F.R.S.-FNRS) under convention 2.5020.11 and by the Walloon Region.
681 We would like to deeply thank the two reviewers and the editor for the careful evaluation
682 of our manuscript and for their constructive comments.

683 Conflict of interest

684 The authors declare that they have no conflict of interest.

685 References

686 Acevedo W, Fallah B, Reich S, Cubasch U (2017) Assimilation of pseudo-
687 Tree-ring-width observations into an atmospheric general circulation model.
688 *Climate of the Past* 13(5):545–557, DOI 10.5194/cp-13-545-2017

- 689 Anchukaitis KJ, Wilson R, Briffa KR, Büntgen U, Cook ER, D'Arrigo R,
690 Davi N, Esper J, Frank D, Gunnarson BE, Hegerl G, Helama S, Klesse
691 S, Krusic PJ, Linderholm HW, Myglan V, Osborn TJ, Zhang P, Rydval
692 M, Schneider L, Schurer A, Wiles G, Zorita E (2017) Last millennium
693 Northern Hemisphere summer temperatures from tree rings: Part II, spa-
694 tially resolved reconstructions. *Quaternary Science Reviews* 163:1–22, DOI
695 10.1016/j.quascirev.2017.02.020
- 696 Anderson DM, Tardif R, Horlick K, Erb MP, Hakim GJ, Noone D, Perkins WA,
697 Steig E (2019) Additions to the Last Millennium Reanalysis Multi-Proxy
698 Database. *Data Science Journal* 18(1):2, DOI 10.5334/dsj-2019-002, URL
699 <https://datascience.codata.org/article/10.5334/dsj-2019-002/>
- 700 Babst F, Bodesheim P, Charney N, Friend AD, Girardin MP, Klesse S, Moore
701 DJ, Seftigen K, Björklund J, Bouriaud O, Dawson A, DeRose RJ, Dietze
702 MC, Eckes AH, Enquist B, Frank DC, Mahecha MD, Poulter B, Record S,
703 Trouet V, Turton RH, Zhang Z, Evans ME (2018) When tree rings go global:
704 Challenges and opportunities for retro- and prospective insight. *Quaternary*
705 *Science Reviews* 197:1–20, DOI 10.1016/j.quascirev.2018.07.009
- 706 Boucher E, Guiot J, Hatté C, Daux V, Danis PA, Dussouillez P (2014) An
707 inverse modeling approach for tree-ring-based climate reconstructions un-
708 der changing atmospheric CO₂ concentrations. *Biogeosciences* 11(12):3245–
709 3258, DOI 10.5194/bg-11-3245-2014
- 710 Breitenmoser P, Brönnimann S, Frank D (2014) Forward modelling of tree-
711 ring width and comparison with a global network of tree-ring chronologies.
712 *Climate of the Past* 10(2):437–449, DOI 10.5194/cp-10-437-2014
- 713 Briffa KR, Schweingruber FH, Jones PD, Osborn TJ, Harris IC, Shiyatov
714 SG, Vaganov EA, Grudd H (1998) Trees tell of past climates: but are they
715 speaking less clearly today? *Philosophical Transactions of the Royal Society*
716 *of London Series B: Biological Sciences* 353(1365):65–73, DOI 10.1098/rstb.
717 1998.0191, URL <https://doi.org/10.1098/rstb.1998.0191>
- 718 Cook ER, Kairiukstis L (1990) *Methods of dendrochronology: Applications*
719 *in the Environmental Sciences*. Kluwer Academic, Boston, DOI 10.1016/
720 0048-9697(91)90076-q
- 721 Danis PA, Hatté C, Misson L, Guiot J (2012) MAIDENiso: a multiproxy bio-
722 physical model of tree-ring width and oxygen and carbon isotopes. *Canadian*
723 *Journal of Forest Research* 42(9):1697–1713, DOI 10.1139/x2012-089, URL
724 <http://www.nrcresearchpress.com/doi/abs/10.1139/x2012-089>
- 725 D'Arrigo R, Wilson R, Liepert B, Cherubini P (2008) On the 'Divergence
726 Problem' in Northern Forests: A review of the tree-ring evidence and pos-
727 sible causes. *Global and Planetary Change* 60(3-4):289–305, DOI 10.1016/
728 j.gloplacha.2007.03.004
- 729 Dee SG, Steiger NJ, Emile-Geay J, Hakim GJ (2016) On the utility of proxy
730 system models for estimating climate states over common era. *Journal of*
731 *Advances in Modeling Earth Systems* 8:1164–1179, DOI [https://doi.org/10.](https://doi.org/10.1002/2016MS000677)
732 [1002/2016MS000677](https://doi.org/10.1002/2016MS000677)
- 733 Drew DM, Downes GM, Battaglia M (2010) CAMBIUM, a process-based
734 model of daily xylem development in Eucalyptus. *Journal of Theoreti-*

- 735 cal Biology 264(2):395–406, DOI 10.1016/j.jtbi.2010.02.013, URL <http://dx.doi.org/10.1016/j.jtbi.2010.02.013>
- 736
- 737 Duchesne L, Houle D, Ouimet R, Caldwell L, Gloor M, Brienen R (2019)
- 738 Large apparent growth increases in boreal forests inferred from tree-rings
- 739 are an artefact of sampling biases. *Scientific Reports* 9(1):1–9, DOI 10.1038/
- 740 s41598-019-43243-1
- 741 Dufrière E, Davi H, François C, Le Maire G, Le Dantec V, Granier A (2005)
- 742 Modelling carbon and water cycles in a beech forest. Part I: Model de-
- 743 scription and uncertainty analysis on modelled NEE. *Ecological Modelling*
- 744 185(2-4):407–436, DOI 10.1016/j.ecolmodel.2005.01.004
- 745 Esper J, George SS, Anchukaitis K, D’Arrigo R, Ljungqvist F, Luter-
- 746 bacher J, Schneider L, Stoffel M, Wilson R, Büntgen U (2018) Large-
- 747 scale, millennial-length temperature reconstructions from tree-rings. *Den-*
- 748 *drochronologia* 50:81–90, DOI 10.1016/j.dendro.2018.06.001, URL <http://linkinghub.elsevier.com/retrieve/pii/S1125786518300687>
- 749
- 750 Evans MN, Tolwinski-Ward SE, Thompson DM, Anchukaitis KJ (2013) Appli-
- 751 cations of proxy system modeling in high resolution paleoclimatology. *Qua-*
- 752 *ternary Science Reviews* 76:16–28, DOI 10.1016/j.quascirev.2013.05.024,
- 753 URL <http://dx.doi.org/10.1016/j.quascirev.2013.05.024>
- 754 Fang M, Li X (2019) An Artificial Neural Networks-Based Tree Ring
- 755 Width Proxy System Model for Paleoclimate Data Assimilation. *Jour-*
- 756 *nal of Advances in Modeling Earth Systems* 11(4):892–904, DOI 10.1029/
- 757 2018MS001525
- 758 FAO/IIASA/ISRIC/ISSCAS/JRC (2012) Harmonized World Soil Database
- 759 (version 1.2). FAO, Rome, Italy and IIASA, Laxenburg, Austria
- 760 Farquhar GD, Caemmerer S, Berry JA (1980) A biochemical model of photo-
- 761 synthetic CO₂ assimilation in leaves of C₃ species. *Planta* 149(1):78–90–90,
- 762 URL <http://dx.doi.org/10.1007/BF00386231>
- 763 Fatichi S, Leuzinger S, Körner C (2014) Moving beyond photosynthesis:
- 764 From carbon source to sink-driven vegetation modeling. *New Phytologist*
- 765 201(4):1086–1095, DOI 10.1111/nph.12614
- 766 Fatichi S, Pappas C, Zscheischler J, Leuzinger S (2019) Modelling carbon
- 767 sources and sinks in terrestrial vegetation. *New Phytologist* 221(2):652–668,
- 768 DOI 10.1111/nph.15451
- 769 Franke J, Brönnimann S, Bhend J, Brugnara Y (2017) A monthly global paleo-
- 770 reanalysis of the atmosphere from 1600 to 2005 for studying past climatic
- 771 variations. *Scientific Data* 4:1–19, DOI 10.1038/sdata.2017.76
- 772 Fritts HC (1976) *Tree rings and climate*. Academic Press, London
- 773 Fritts HC (1991) *Reconstructing large-scale climatic patterns from tree-ring*
- 774 *data: A diagnostic analysis*. University of Arizona Press, Tucson, Arizona,
- 775 USA
- 776 Gea-Izquierdo G, Guibal F, Joffre R, Ourcival JM, Simioni G, Guiot J (2015)
- 777 Modelling the climatic drivers determining photosynthesis and carbon allo-
- 778 cation in evergreen Mediterranean forests using multiproxy long time series.
- 779 *Biogeosciences* 12(3):2745–2786, DOI 10.5194/bgd-12-2745-2015

- 780 Gea-Izquierdo G, Nicault A, Battipaglia G, Dorado-Liñán I, Gutiérrez E,
781 Ribas M, Guiot J (2017) Risky future for Mediterranean forests unless they
782 undergo extreme carbon fertilization. *Global Change Biology* 23(7):2915–
783 2927, DOI 10.1111/gcb.13597, 0608246v3
- 784 Gennaretti F, Gea-Izquierdo G, Boucher E, Berninger F, Arseneault D, Guiot
785 J (2017) Ecophysiological modeling of the climate imprint on photosynthesis
786 and carbon allocation to the tree stem in the North American boreal forest.
787 *Biogeosciences* 14:4851–4866, DOI 10.5194/bg-2017-51
- 788 Giguère-Croteau C, Boucher É, Bergeron Y, Girardin MP, Drobyshev I, Silva
789 LC, Hélie JF, Garneau M (2019) Correction: Plant biology, earth, atmo-
790 spheric, and planetary sciences (Proceedings of the National Academy of
791 Sciences of the United States of America (2019) 116 (2749–2754) DOI:
792 10.1073/pnas.1816686116). *Proceedings of the National Academy of Sci-*
793 *ences of the United States of America* 116(10):4748, DOI 10.1073/pnas.
794 1902083116
- 795 Girardin MP, Bouriaud O, Hogg EH, Kurz W, Zimmermann NE, Metsaranta
796 JM, De Jong R, Frank DC, Esper J, Büntgen U, Guo XJ, Bhatti J (2016) No
797 growth stimulation of Canada’s boreal forest under half-century of combined
798 warming and CO₂ fertilization. *Proceedings of the National Academy of*
799 *Sciences of the United States of America* 113(52):E8406–E8414, DOI 10.
800 1073/pnas.1610156113
- 801 Goosse H, Crespin E, Dubinkina S, Loutre MF, Mann ME, Renssen H, Sallaz-
802 Damaz Y, Shindell D (2012) The role of forcing and internal dynamics in ex-
803 plaining the "Medieval Climate Anomaly". *Climate Dynamics* 39(12):2847–
804 2866, DOI 10.1007/s00382-012-1297-0
- 805 Guiot J, Torre F, Jolly D, Peyron O, Boreux JJ, Cheddadi R (2000) Inverse
806 vegetation modeling by Monte Carlo sampling to reconstruct palaeoclimates
807 under changed precipitation seasonality and CO₂ conditions: Application to
808 glacial climate in Mediterranean region. *Ecological Modelling* 127(2-3):119–
809 140, DOI 10.1016/S0304-3800(99)00219-7
- 810 Guiot J, Boucher E, Gea-Izquierdo G (2014) Process models and model-data
811 fusion in dendroecology. *Frontiers in Ecology and Evolution* 2:1–12, DOI 10.
812 3389/fevo.2014.00052, URL [http://journal.frontiersin.org/article/
813 10.3389/fevo.2014.00052/abstract](http://journal.frontiersin.org/article/10.3389/fevo.2014.00052/abstract)
- 814 Hararuk O, Campbell EM, Antos JA, Parish R (2019) Tree rings provide
815 no evidence of a CO₂ fertilization effect in old-growth subalpine forests of
816 western Canada. *Global Change Biology* 25(4):1222–1234, DOI 10.1111/gcb.
817 14561
- 818 Hartig F, Minunno F, Paul S (2019) BayesianTools: General-Purpose MCMC
819 and SMC Samplers and Tools for Bayesian Statistics. R package version
820 0.1.6. URL <https://github.com/florianhartig/BayesianTools>
- 821 Hunter JD (2007) Matplotlib: A 2D graphics environment. *Computing in Sci-*
822 *ence and Engineering* 9(3):90–95, DOI 10.1109/MCSE.2007.55
- 823 Jones PD, Briffa KR, Barnett TP, Tett SFB (1998) High-resolution palaeocli-
824 matic records for the last millennium. *The Holocene* 4:455–471

- 825 Jones PD, Briffa KR, Osborn TJ, Lough JM, Van Ommen TD, Vinther BM,
826 Luterbacher J, Wahl ER, Zwiens FW, Mann ME, Schmidt GA, Ammann
827 CM, Buckley BM, Cobb KM, Esper J, Goosse H, Graham N, Jansen E,
828 Kiefer T, Kull C, Küttel M, Mosley-Thompson E, Overpeck JT, Riedwyl
829 N, Schulz M, Tudhope AW, Villalba R, Wanner H, Wolff E, Xoplaki E
830 (2009) High-resolution palaeoclimatology of the last millennium: A review
831 of current status and future prospects. *Holocene* 19(1):3–49, DOI 10.1177/
832 0959683608098952
- 833 Konecky B, McKay N, Churakova (Sidorova) O, Comas-Bru L, Dassié E, De-
834 Long K, Falster G, Fischer M, Jones M, Jonkers L, Kaufman D, Leduc G,
835 Managave S, Martrat B, Opel T, Orsi A, Partin J, Sayani H, Thomas E,
836 Thompson D, Tyler J, Abram N, Atwood A, Conroy J, Kern Z, Porter T,
837 Stevenson S, von Gunten L (2020) The Iso2k Database: A global compilation
838 of paleo- $\delta^{18}\text{O}$ and $\delta^2\text{H}$ records to aid understanding of Common Era climate.
839 *Earth System Science Data* (12):2261–2288, DOI 10.5194/essd-12-2261-2020
- 840 Körner C (2015) Paradigm shift in plant growth control. *Current Opinion in*
841 *Plant Biology* 25:107–114, DOI 10.1016/j.pbi.2015.05.003
- 842 Körner C, Asshoff R, Bignucolo O, Hättenschwiler S, Keel SG, Peláez-
843 Riedl S, Pepin S, Siegwolf RT, Zotz G (2005) Ecology: Carbon flux and
844 growth in mature deciduous forest trees exposed to elevated CO_2 . *Science*
845 309(5739):1360–1362, DOI 10.1126/science.1113977
- 846 Lavergne A, Daux V, Villalba R, Barichivich J (2015) Temporal changes
847 in climatic limitation of tree-growth at upper treeline forests: Contrasted
848 responses along the west-to-east humidity gradient in Northern Patago-
849 nia. *Dendrochronologia* 36:49–59, DOI 10.1016/j.dendro.2015.09.001, URL
850 <http://dx.doi.org/10.1016/j.dendro.2015.09.001>
- 851 Lavergne A, Gennaretti F, Risi C, Daux V, Savard M, Naulier M, Villalba R,
852 Begin C, Lavergne A, Gennaretti F, Risi C, Daux V, Boucher E, Lavergne
853 A, Gennaretti F, Risi C, Daux V, Boucher E, Savard MM (2017) Modelling
854 tree ring cellulose $\delta^{18}\text{O}$ variations in two temperature-sensitive tree species
855 from North and South America. *Climate of the Past* (13):1515–1526
- 856 Leuning R (1995) A critical appraisal of a combined stomatal-
857 photosynthesis model for C_3 plants. *Plant, Cell & Environment* 18(4):339–
858 355, DOI <https://doi.org/10.1111/j.1365-3040.1995.tb00370.x>, URL
859 [https://onlinelibrary.wiley.com/doi/abs/10.1111/j.1365-3040.](https://onlinelibrary.wiley.com/doi/abs/10.1111/j.1365-3040.1995.tb00370.x)
860 [1995.tb00370.x](https://onlinelibrary.wiley.com/doi/abs/10.1111/j.1365-3040.1995.tb00370.x)
- 861 Lévesque M, Siegwolf R, Saurer M, Eilmann B, Rigling A (2014) Increased
862 water-use efficiency does not lead to enhanced tree growth under xeric and
863 mesic conditions. *New Phytologist* 203(1):94–109, DOI 10.1111/nph.12772
- 864 Mann ME, Bradley RS, Hughes MK (1999) Northern Hemisphere tempera-
865 tures during the past millennium. *Climate Change: Evaluating recent and*
866 *future climate change* 26(6):759–762
- 867 Mann ME, Zhang Z, Hughes MK, Bradley RS, Miller SK, Rutherford S, Ni F
868 (2008) Proxy-based reconstructions of hemispheric and global surface tem-
869 perature variations over the past two millennia. *Proceedings of the National*
870 *Academy of Sciences* 105(36):13252–13257, DOI 10.1073/pnas.0805721105

- 871 Mann ME, Zhang Z, Rutherford S, Bradley RS, Hughes MK, Shindell D, Am-
872 mann C, Faluvegi G, Ni F (2009) Global Signatures and Dynamical Origins
873 of the Little Ice Age and Medieval Climate Anomaly. *Science* 326:1256–1260,
874 DOI 10.1126/science.1166349
- 875 Marchand W, Girardin MP, Hartmann H, Depardieu C, Isabel N, Gauthier
876 S, Boucher É, Bergeron Y (2020) Strong overestimation of water-use effi-
877 ciency responses to rising CO₂ in tree-ring studies. *Global Change Biology*
878 26(8):4538–4558, DOI 10.1111/gcb.15166
- 879 Misson L (2004) MAIDEN: a model for analyzing ecosystem processes in
880 dendroecology. *Canadian Journal of Forest Research* 34(4):874–887, DOI
881 10.1139/x03-252, URL [http://www.nrcresearchpress.com/doi/abs/10.](http://www.nrcresearchpress.com/doi/abs/10.1139/x03-252)
882 [1139/x03-252](http://www.nrcresearchpress.com/doi/abs/10.1139/x03-252)
- 883 Myhre G, Shindell D, Bréon FM, Collins W, Fuglestedt J, Huang J, Koch
884 D, Lamarque JF, Lee D, Mendoza B, Nakajima T, Robock A, Stephens G,
885 Takemura T, Zhang H (2013) Anthropogenic and Natural Radiative Forc-
886 ing. In: *Climate Change 2013: The Physical Science Basis. Contribution of*
887 *Working Group I to the Fifth Assessment Report of the Intergovernmental*
888 *Panel on Climate Change*, Cambridge University Press, Cambridge, United
889 Kingdom and New York, USA., DOI 10.1017/CBO9781107415324.018
- 890 PAGES 2k Consortium (2013) Continental-scale temperature variability dur-
891 ing the past two millennia. *Nature Geoscience* 6(5):339–346, DOI 10.1038/
892 ngeo1797
- 893 PAGES 2k Consortium (2017) A global multiproxy database for temperature
894 reconstructions of the Common Era. *Scientific Data* 4(170088):1–33, DOI
895 DOI:10.1038/sdata.2017.88
- 896 Peñuelas J, Canadell JG, Ogaya R (2011) Increased water-use efficiency during
897 the 20th century did not translate into enhanced tree growth. *Global Ecology*
898 *and Biogeography* 20(4):597–608, DOI 10.1111/j.1466-8238.2010.00608.x
- 899 Rezsöhazy J, Goosse H, Guiot J, Gennaretti F, Boucher E, André F, Jonard
900 M (2020) Application and evaluation of the dendroclimatic process-based
901 model MAIDEN during the last century in Canada and Europe. *Climate of*
902 *The Past* 16:1043–1059, DOI 10.5194/cp-16-1043-2020
- 903 Seftigen K, Frank DC, Björklund J, Babst F, Poulter B (2018) The climatic
904 drivers of normalized difference vegetation index and tree-ring-based esti-
905 mates of forest productivity are spatially coherent but temporally decou-
906 pled in Northern Hemispheric forests. *Global Ecology and Biogeography*
907 27(11):1352–1365, DOI 10.1111/geb.12802
- 908 Sheffield J, Goteti G, Wood EF (2006) Development of a 50-year high-
909 resolution global dataset of meteorological forcings for land surface mod-
910 eling. *Journal of Climate* 19(13):3088–3111, DOI 10.1175/JCLI3790.1
- 911 Silva LC, Anand M, Leithead MD (2010) Recent widespread tree growth de-
912 cline despite increasing atmospheric CO₂. *PLoS ONE* 5(7), DOI 10.1371/
913 journal.pone.0011543
- 914 St George S, Esper J (2019) Concord and discord among Northern Hemisphere
915 paleotemperature reconstructions from tree rings. *Quaternary Science Re-*
916 *views* 203:278–281, DOI S0277379118307170

- 917 Steiger NJ, Smerdon JE (2017) A pseudoproxy assessment of data as-
918 simulation for reconstructing the atmosphere-ocean dynamics of hydro-
919 climate extremes. *Climate of the Past* 13(10):1435–1449, DOI 10.5194/
920 cp-13-1435-2017
- 921 Steiger NJ, Smerdon JE, Cook ER, Cook BI (2018) A reconstruction of global
922 hydroclimate and dynamical variables over the Common Era. *Scientific Data*
923 5:1–15, DOI 10.1038/sdata.2018.86
- 924 Tardif R, Hakim GJ, Perkins WA, Horlick KA, Erb MP, Emile-Geay J, An-
925 derson DM, Steig EJ, Noone D (2019) Last Millennium Reanalysis with an
926 expanded proxy database and seasonal proxy modeling. *Climate of the Past*
927 15(4):1251–1273, DOI 10.5194/cp-15-1251-2019
- 928 Tolwinski-Ward SE, Evans MN, Hughes MK, Anchukaitis KJ (2011) An
929 efficient forward model of the climate controls on interannual variation
930 in tree-ring width. *Climate Dynamics* 36(11-12):2419–2439, DOI 10.1007/
931 s00382-010-0945-5
- 932 Tolwinski-Ward SE, Anchukaitis KJ, Evans MN (2013) Bayesian parameter
933 estimation and interpretation for an intermediate model of tree-ring width.
934 *Climate of the Past* 9(4):1481–1493, DOI 10.5194/cp-9-1481-2013
- 935 Vaganov EA, Hughes MK, Shashkin A (2006) Growth dynamics of conifer tree
936 rings, Springer edn. New York
- 937 Van Der Sleen P, Groenendijk P, Vlam M, Anten NP, Boom A, Bongers F,
938 Pons TL, Terburg G, Zuidema PA (2015) No growth stimulation of tropical
939 trees by 150 years of CO₂ fertilization but water-use efficiency increased.
940 *Nature Geoscience* 8(1):24–28, DOI 10.1038/ngeo2313
- 941 Wilson R, Elling W (2004) Temporal instability in tree-growth/climate re-
942 sponse in the Lower Bavarian Forest region: Implications for dendrocli-
943 matic reconstruction. *Trees - Structure and Function* 18(1):19–28, DOI
944 10.1007/s00468-003-0273-z
- 945 Wilson R, D’Arrigo R, Buckley B, Büntgen U, Esper J, Frank D, Luckman B,
946 Payette S, Vose R, Youngblut D (2007) A matter of divergence: Tracking
947 recent warming at hemispheric scales using tree ring data. *Journal of Geo-
948 physical Research Atmospheres* 112(17):1–17, DOI 10.1029/2006JD008318
- 949 Wilson R, Anchukaitis K, Briffa KR, Büntgen U, Cook E, D’Arrigo R, Davi N,
950 Esper J, Frank D, Gunnarson B, Hegerl G, Helama S, Klesse S, Krusic PJ,
951 Linderholm HW, Myglan V, Osborn TJ, Rydval M, Schneider L, Schurer
952 A, Wiles G, Zhang P, Zorita E (2016) Last millennium northern hemisphere
953 summer temperatures from tree rings: Part I: The long term context. *Qua-
954 ternary Science Reviews* 134:1–18, DOI 10.1016/j.quascirev.2015.12.005

S1 Supplementary materials

Table S1 Main constants linked to site conditions and control parameters in the MAIDEN model.

Parameter	Meaning	Units
<i>exp_site</i>	Indicates if the species at the site is a deciduous (1) or ever-green (2) tree	no unit (1 or 2)
<i>base_elev_cst</i>	Station elevation	meters
<i>base_isoh_cst</i>	Station isohyet	centimeters
<i>site_lat_cst</i>	Site latitude	degrees
<i>site_elev_cst</i>	Site elevation	meters
<i>site_slp_cst</i>	Site slope	degrees
<i>site_asp_cst</i>	Site aspect	degrees
<i>site_isoh_cst</i>	Site isohyet	centimeters
<i>site_ehoriz_cst</i>	Site East slope	degrees
<i>site_whoriz_cst</i>	Site West slope	degrees
<i>thick1-2-3 or 4</i>	Soil layer thickness	meters
<i>finefrac1-2-3 or 4</i>	% of fine roots in the soil layer	Coeff. between 0-1
<i>clay1-2-3 or 4</i>	% of clay in the soil layer	%
<i>sand1-2-3 or 4</i>	% of sand in the soil layer	%

Table S2 Calibrated parameters of the MAIDEN model (Gennaretti et al., 2017).

	Process		Parameter	Units
Photosynthesis	Temperature dependence of photosynthesis	Asymptote	V_{max}	$\mu\text{mol C}\cdot\text{m}^{-2}$ of leaves \cdot s^{-1}
		Slope	V_b	$^{\circ}\text{C}^{-1}$
		Inflection point	V_{ip}	$^{\circ}\text{C}$
	Water stress dependence of stomatal conductance	Slope	$soil_b$	mm^{-1}
		Inflection point	$soil_{ip}$	mm
	Acclimation to temperature of photosynthesis	Needed days	τ	days
Carbon allocation	Definition of canopy maximum amount of carbon	Slope of temperature dependence	$CanopyT$	$^{\circ}\text{C}^{-1}$
		Slope of precipitation dependence	$CanopyP$	mm^{-1}
	Start of the growing season (budburst)	GDD sum threshold	GDD_1	$^{\circ}\text{C}$
		Day before the later start	$vegphase23$	day of the year
		Acclimation to changing GDD sums	$day23_flex$	years
	Daily available carbon from buds reservoir	Storage C used by the tree	C_{bud}	$\text{gC}\cdot\text{m}^{-2}$ of stand \cdot day^{-1}
	Partition of carbon to different tree compartments during growing season	Portion allocated to canopy and roots	$h3$	fraction (0-1)
		Inflection point of the temperature dependence	st_{temp}	$^{\circ}\text{C}$
	Partition of carbon to different tree compartments during summer period	Photoperiod threshold	$photoper$	hours
	Photoperiod for transition from summer to fall season	Yearly canopy turnover rate	$PercentFall$	fraction (0-1)
	Carbon losses from the canopy (evergreen only)	Approximate day of the year with maximum losses	$OutMax$	day of the year
		Index proportional to the length of the period with losses	$OutLength$	NA

Table S3 Calibrated parameters of the MAIDEN model (Gea-Izquierdo et al., 2015).

	Process		Parameter	Units
Photosynthesis	Temperature dependence of photosynthesis	Asymptote	V_{max}	$\mu\text{mol C.m}^{-2}$ of leaves . s^{-1}
		Slope	V_b	$^{\circ}\text{C}^{-1}$
		Inflection point	V_{ip}	$^{\circ}\text{C}$
	Water stress dependence of stomatal conductance	Slope	$soil_b$	mm^{-1}
		Inflection point	$soil_{ip}$	mm
Carbon allocation	Definition of canopy maximum amount of carbon	Slope of temperature dependence	$perc_{LAI}$	$^{\circ}\text{C}^{-1}$
	Start of the growing season (budburst)	GDD sum threshold	GDD_1	$^{\circ}\text{C}$
		Day before the later start	$vegphase23$	day of the year
	Daily available carbon from buds reservoir	Storage C used by the tree	C_{bud}	gC.m^{-2} of stand . day^{-1}
	Partition of carbon to different tree compartments during growing season	Definition of carbon allocated to the stem as a function of soil water	$p3moist$	mm^{-1}
		Definition of carbon allocated to the stem as a function of maximum temperature	$p3temp$	$^{\circ}\text{C}$
		Definition of carbon allocated to the stem as a function of soil water	$p3sd$	$^{\circ}\text{C}$
		Definition of carbon allocated to the stem as a function of soil water	$st3moist$	mm^{-1}
		Definition of carbon allocated to the stem as a function of maximum temperature	$st3temp$	$^{\circ}\text{C}$
		Definition of carbon allocated to the stem as a function of maximum temperature	$st3sd_temp$	$^{\circ}\text{C}$
	Partition of carbon to different tree compartments during summer period	Definition of carbon allocated to stem or storage as a function of maximum temperature	$st4temp$	$^{\circ}\text{C}^{-1}$
		Definition of carbon allocated to stem or storage as a function of soil water	$st4sd_moist$	mm
	Photoperiod for transition from summer to fall season	Photoperiod threshold	$photoper$	hours

Table S4 Ranges of calibrated parameters prior uniform distributions, for the MAIDEN model (Gennaretti et al., 2017). See Table S2 for details on calibrated parameters.

	Parameter	Lower bound	Upper bound
Photosynthesis	V_{max}	5	150
	V_b	-0.3	-0.05
	V_{ip}	5	30
	$soil_b$	-0.06	-0.005
	$soil_{ip}$	3	400
	τ	1	20
Carbon allocation	$CanopyT$	0	20
	$CanopyP$	0	20
	GDD_1	10	250
	$vegphase23$	90	190
	$day23_flex$	1	10
	C_{bud}	1	16
	$h3$	0	1
	st_{temp}	1	100
	$photoper$	9	14
	$PercentFall$	0.09	0.5
	$OutMax$	120	250
	$OutLength$	2	15

Table S5 Ranges of calibrated parameters prior uniform distributions, for the MAIDEN model (Gea-Izquierdo et al., 2015). See Table S3 for details on calibrated parameters.

	Parameter	Lower bound	Upper bound
Photosynthesis	V_{max}	5	150
	V_b	-0.3	-0.05
	V_{ip}	5	30
	$soil_b$	-0.06	-0.005
	$soil_{ip}$	3	400
Carbon allocation	$perc_{LAI}$	40	250
	GDD_1	10	250
	$vegphase23$	90	190
	C_{bud}	1	16
	p_{3moist}	-0.7	-0.001
	p_{3temp}	-160	185
	p_{3sd}	5	200
	st_{3moist}	-0.8	-0.005
	st_{3temp}	-170	230
	st_{3sd_temp}	5	300
	st_{4temp}	0.008	0.95
	st_{4sd_moist}	45	1090
	$photoper$	9	14

Table S6 Pearson correlations between different climate indicators and MAIDEN or VS-Lite verification correlations (1901-1949). O-S stands for the year starting from October (previous year) to September (current year); P for precipitation; JAS for July-August-September; T for temperature. Asterisks stand for significant correlations (p-value < 0.05). The difference in the number of sites on which correlations are computed is due to the phenological criterion that has been applied to MAIDEN calibrated sites (see Sect. 2.4.1 for more details).

Model (version)	Correlation
Correlations between O-S mean cumulative P correlation and verification correlation	
MAIDEN (Ge2017; 189 sites)	0.073
MAIDEN (GI2015; 160 sites)	0.076
VS-Lite (302 sites)	-0.067
Correlations between annual mean T correlation and verification correlation	
MAIDEN (Ge2017; 189 sites)	0.036
MAIDEN (GI2015; 160 sites)	0.036
VS-Lite (302 sites)	-0.052
Correlations between JAS mean T correlation and verification correlation	
MAIDEN (Ge2017; 189 sites)	0.027
MAIDEN (GI2015; 160 sites)	0.049
VS-Lite (302 sites)	-0.053

Table S7 Pearson correlations between correlations of observed TRW with different climate indicators and MAIDEN or VS-Lite verification correlations (1901-1949). O-S stands for the year starting from October (previous year) to September (current year); P for precipitation; JAS for July-August-September; T for temperature. Asterisks stand for significant correlations (p-value < 0.05). The difference in the number of sites on which correlations are computed is due to the phenological criterion that has been applied to MAIDEN calibrated sites (see Sect. 2.4.1 for more details).

Model (version)	Correlation
Correlations between observed TRW and O-S P correlation and verification correlation	
MAIDEN (Ge2017; 189 sites)	0.114
MAIDEN (GI2015; 160 sites)	0.155
VS-Lite (302 sites)	0.149*
VS-Lite (189 Ge2017 selected sites)	0.190*
VS-Lite (160 GI2015 selected sites)	0.091
Correlations between observed TRW and annual T correlation and verification correlation	
MAIDEN (Ge2017; 189 sites)	0.074
MAIDEN (GI2015; 160 sites)	0.059
VS-Lite (302 sites)	0.467*
VS-Lite (189 Ge2017 selected sites)	0.471*
VS-Lite (160 GI2015 selected sites)	0.503*
Correlations between observed TRW and JAS T correlation and verification correlation	
MAIDEN (Ge2017; 189 sites)	-0.039
MAIDEN (GI2015; 160 sites)	-0.097
VS-Lite (302 sites)	0.506*
VS-Lite (189 Ge2017 selected sites)	0.496*
VS-Lite (160 GI2015 selected sites)	0.494*

Table S8 Pearson correlations of correlations between different climate indicators and tree-ring width observations with correlations between the same climate indicators and MAIDEN or VS-Lite tree-growth simulations (1901-1949 verification period). O-S stands for the year starting from October (previous year) to September (current year); P for precipitation; JAS for July-August-September; T for temperature; TRindex for tree-ring index. Asterisks stand for significant correlations (p-value < 0.05). The difference in the number of sites on which correlations are computed is due to the phenological criterion that has been applied to MAIDEN calibrated sites (see Sect. 2.4.1 for more details).

Model (version)	Correlation
Correlations between observed TRW and O-S P correlation and simulated TRindex and O-S P correlation	
MAIDEN (Ge2017; 189 sites)	0.388*
MAIDEN (GI2015; 160 sites)	0.322*
VS-Lite (302 sites)	0.515*
VS-Lite (189 Ge2017 selected sites)	0.552*
VS-Lite (160 GI2015 selected sites)	0.552*
MAIDEN (well-fitted sites only)	0.694*
VS-Lite (well-fitted sites only)	0.837*
MAIDEN (common well-fitted sites only)	0.747*
VS-Lite (common well-fitted sites only)	0.886*
Correlations between observed TRW and annual T correlation and simulated TRindex and annual T correlation	
MAIDEN (Ge2017; 189 sites)	0.053
MAIDEN (GI2015; 160 sites)	0.171*
VS-Lite (302 sites)	0.241*
VS-Lite (189 Ge2017 selected sites)	0.203*
VS-Lite (160 GI2015 selected sites)	0.291*
MAIDEN (well-fitted sites only)	0.648*
VS-Lite (well-fitted sites only)	0.678*
MAIDEN (common well-fitted sites only)	0.608*
VS-Lite (common well-fitted sites only)	0.772*
Correlations between observed TRW and JAS T correlation and simulated TRindex and JAS T correlation	
MAIDEN (Ge2017; 189 sites)	0.130
MAIDEN (GI2015; 160 sites)	0.216*
VS-Lite (302 sites)	0.338*
VS-Lite (189 Ge2017 selected sites)	0.329*
VS-Lite (160 GI2015 selected sites)	0.328*
MAIDEN (well-fitted sites only)	0.759*
VS-Lite (well-fitted sites only)	0.704*
MAIDEN (common well-fitted sites only)	0.739*
VS-Lite (common well-fitted sites only)	0.787*

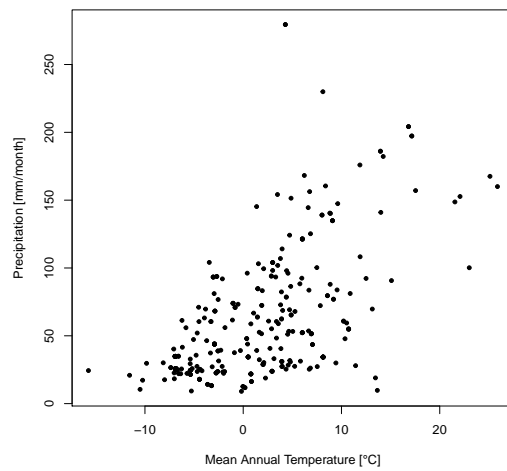


Fig. S1 Mean monthly cumulative precipitation (in millimeters per month) as a function of mean annual temperature (in °C) at the 302 PAGES2k TRW sites used in this study. The climate data are from the *Global Meteorological Forcing Dataset for land surface modelling (v2)* at 0.5° resolution (Section 2.3) over the 1901-2000 time period.

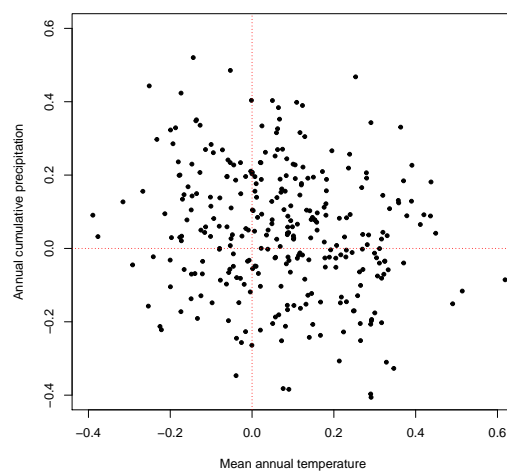


Fig. S2 Correlations between annual cumulative precipitation and TRW observations as a function of correlations between mean annual temperature and TRW observations at the 302 PAGES2k TRW sites used in this study, over the 1901-2000 period. The climate data are from the *Global Meteorological Forcing Dataset for land surface modelling (v2)* at 0.5° resolution (Section 2.3).

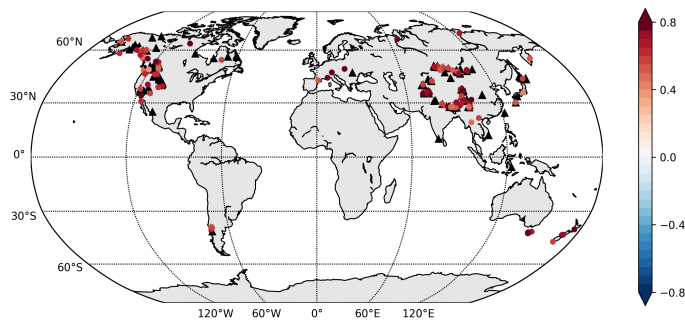


Fig. S3 MAIDEN (Gea-Izquierdo et al., 2015) calibration correlations for selected sites (Sect. 2.4.1; 160 sites out of 302). Background map from Hunter (2007).

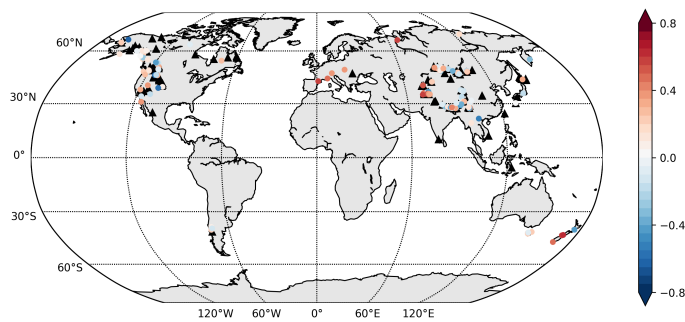


Fig. S4 MAIDEN (Gea-Izquierdo et al., 2015) verification correlations for selected sites (Sect. 2.4.1; 160 sites out of 302). Background map from Hunter (2007).

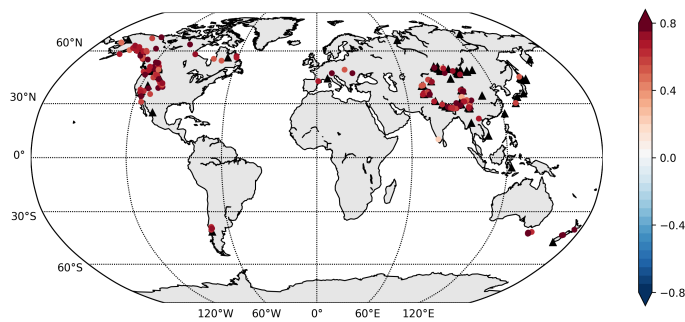


Fig. S5 MAIDEN (Gennaretti et al., 2017) calibration correlations for selected sites (Sect. 2.4.1; 189 sites out of 302). Background map from Hunter (2007).

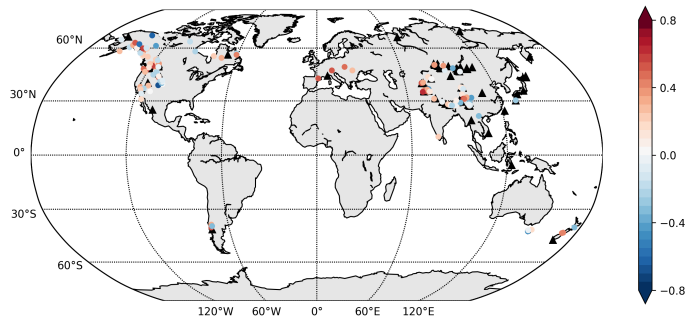


Fig. S6 MAIDEN (Gennaretti et al., 2017) verification correlations for selected sites (Sect. 2.4.1; 189 sites out of 302). Background map from Hunter (2007).

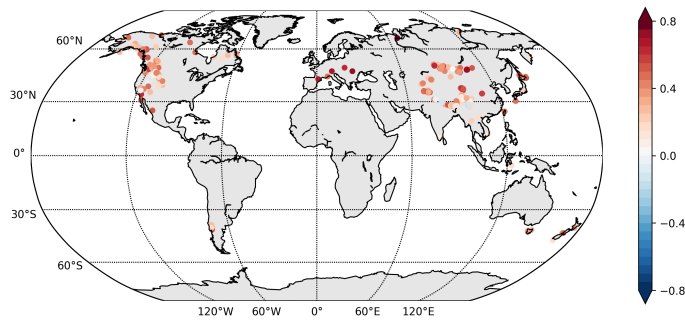


Fig. S7 VS-Lite calibration correlations for 302 sites. Background map from Hunter (2007).

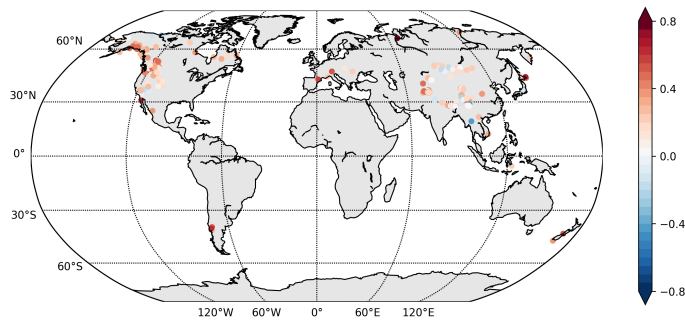
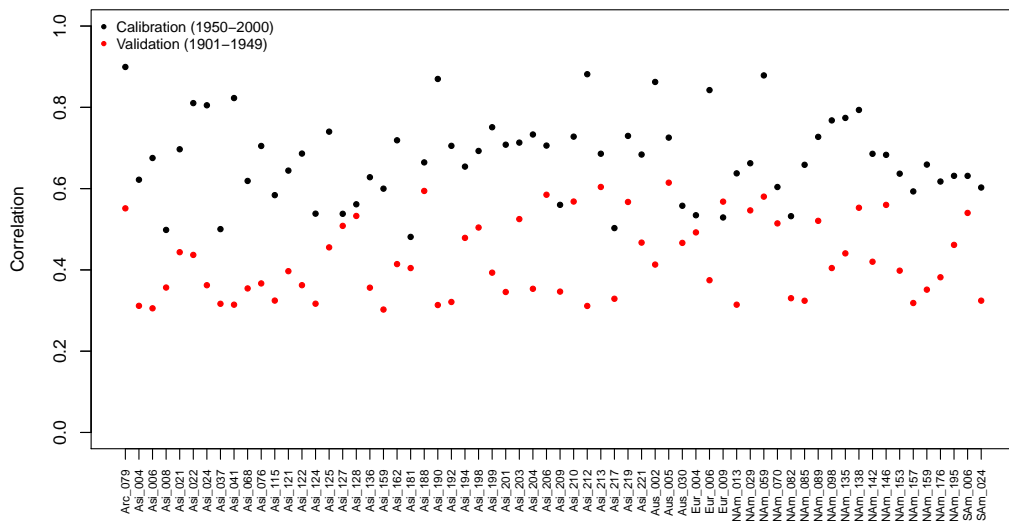
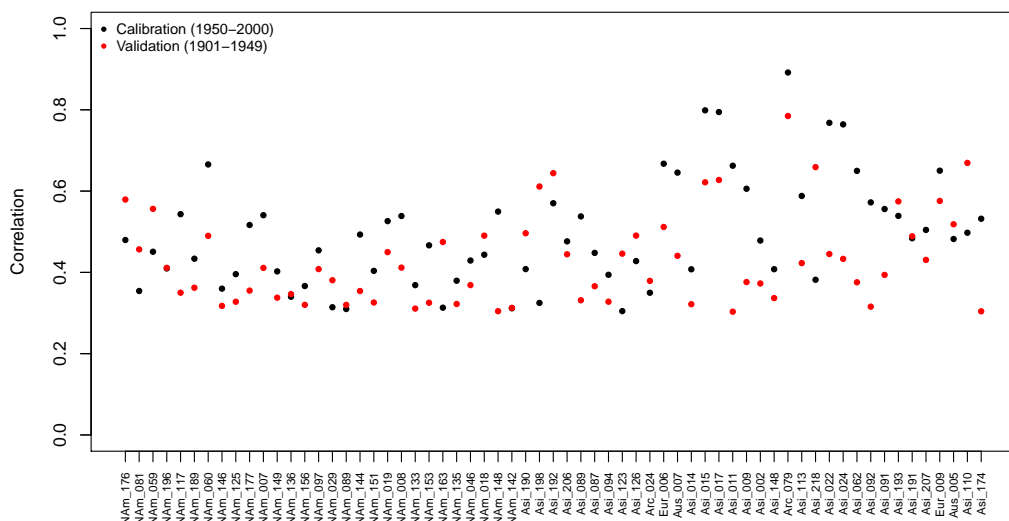


Fig. S8 VS-Lite verification correlations for 302 sites. Background map from Hunter (2007).



(a) MAIDEN



(b) VS-Lite

Fig. S9 (a) MAIDEN (64 sites) and (b) VS-Lite (63 sites) calibration (1950-2000) and verification (1901-1949) correlations (all significant at the 95% confidence level) for well-fitted sites (Sect. 3.1) (with names from the PAGES2k database: *NAm* for North American sites; *Asi* for Asian sites; *Eur* for European sites; *Arc* for Arctic sites; *Aus* for Australian, Tasmanian or New Zealand sites; *Sam* for South American sites).

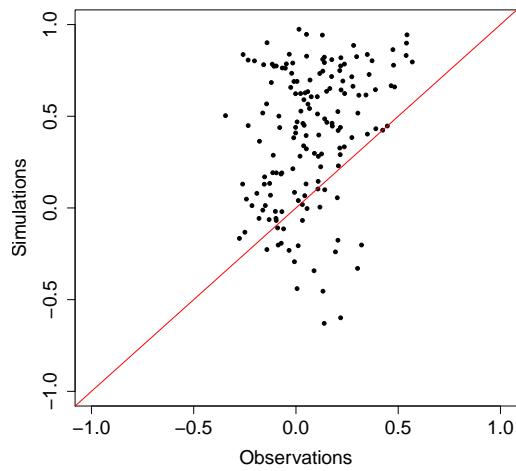


Fig. S10 Correlations between mean annual temperature and VS-Lite tree-ring index simulations as a function of correlations between mean annual temperature and TRW observations for MAIDEN (Gea-Izquierdo et al., 2015) selected sites (Sect. 2.4.1; 160 sites out of 302), over the 1901-1949 verification period.

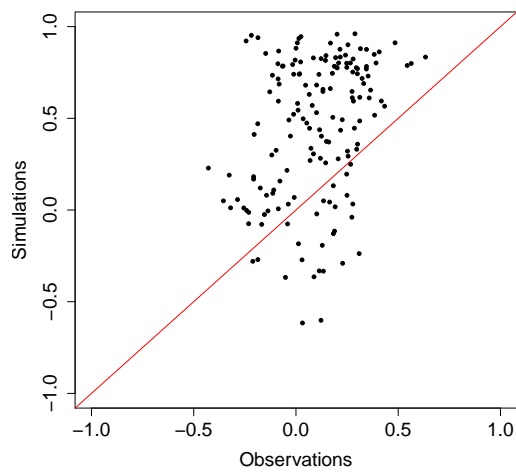


Fig. S11 Correlations between mean July-August-September temperature and VS-Lite tree-ring index simulations as a function of correlations between mean July-August-September temperature and TRW observations for MAIDEN (Gea-Izquierdo et al., 2015) selected sites (Sect. 2.4.1; 160 sites out of 302), over the 1901-1949 verification period.

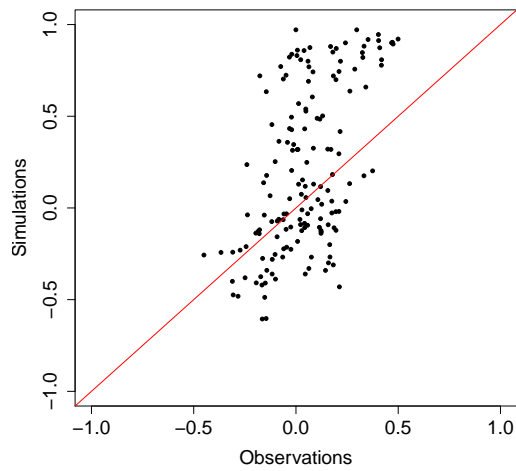


Fig. S12 Correlations between October-September cumulative precipitation and VS-Lite tree-ring index simulations as a function of correlations between October-September cumulative precipitation and TRW observations for MAIDEN (Gea-Izquierdo et al., 2015) selected sites (Sect. 2.4.1; 160 out of 302), over the 1901-1949 verification period.

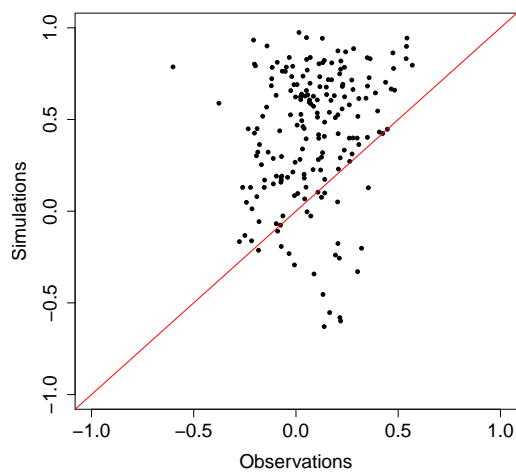


Fig. S13 Correlations between mean annual temperature and VS-Lite tree-ring index simulations as a function of correlations between mean annual temperature and TRW observations for MAIDEN (Gennaretti et al., 2017) selected sites (Sect. 2.4.1; 189 sites out of 302), over the 1901-1949 verification period.

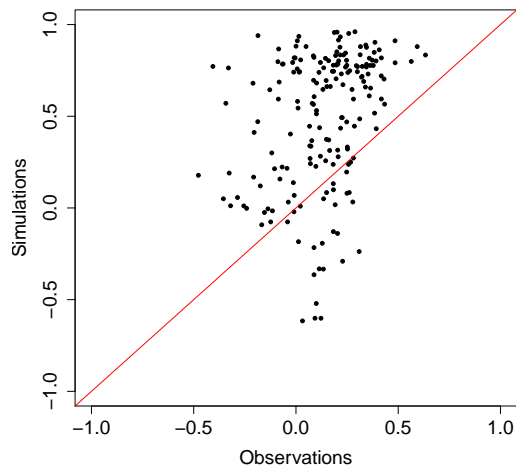


Fig. S14 Correlations between mean July-August-September temperature and VS-Lite tree-ring index simulations as a function of correlations between mean July-August-September temperature and TRW observations for MAIDEN (Gennaretti et al., 2017) selected sites (Sect. 2.4.1; 189 sites out of 302), over the 1901-1949 verification period.

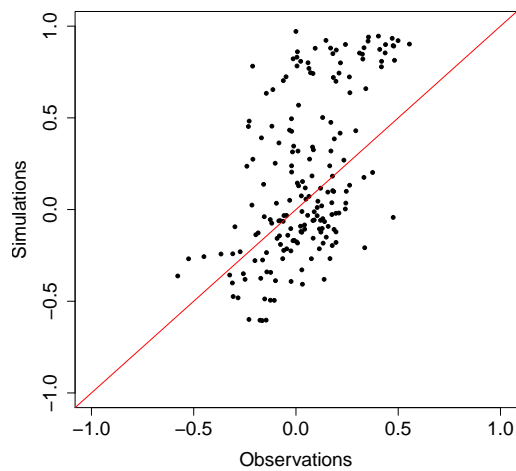


Fig. S15 Correlations between October-September cumulative precipitation and VS-Lite tree-ring index simulations as a function of correlations between October-September cumulative precipitation and TRW observations for MAIDEN (Gennaretti et al., 2017) selected sites (Sect. 2.4.1; 189 out of 302), over the 1901-1949 verification period.